Genetic effects on promoter usage are highly context-specific and contribute to complex traits

Kaur Alasoo[1,2], Julia Rodrigues[2], John Danesh[2-5], Daniel F. Freitag[2-4], Dirk S. Paul[2-4,#], Daniel J. Gaffney[2,#]

[1]Institute of Computer Science, University of Tartu, 51009, Tartu, Estonia
[2]Wellcome Sanger Institute, Wellcome Genome Campus, Hinxton, Cambridge CB10 1SA, UK.
[3]BHF Cardiovascular Epidemiology Unit, Department of Public Health and Primary Care, University of Cambridge, Cambridge CB1 8RN, UK.
[4]British Heart Foundation Centre of Excellence, Division of Cardiovascular Medicine, Addenbrooke's Hospital, Cambridge CB2 0QQ, UK.
[5]National Institute for Health Research Blood and Transplant Unit (NIHR BTRU) in Donor Health and Genomics, Department of Public Health and Primary Care, University of Cambridge, Cambridge CB1 8RN, UK.
[#] jointly supervised the study

Corresponding author: Kaur Alasoo (kaur.alasoo@ut.ee)

Abstract

Genetic variants regulating RNA splicing and transcript usage have been implicated in both common and rare diseases. However, identifying specific transcriptional effects of these variants remains challenging, partly because reference transcriptomes are incomplete and contain many truncated transcripts that lack annotated 3' or 5' ends. We developed a novel analytical approach to overcome these limitations by stratifying transcript annotations into three separate components: promoters, internal exons and 3' ends. We apply our method to genotype and RNA-seq data from human macrophages exposed to a range of inflammatory stimuli (IFNɣ, *Salmonella*, IFNɣ + *Salmonella*) and a metabolic stimulus (acetylated LDL), obtained from up to 84 individuals. We found that over half of the quantitative trait loci (QTLs) colocalising with complex traits were identified only at the transcript level with no detectable effect on total gene expression. Furthermore, 55% of the transcript-level associations regulated either promoter or 3' end usage, many of which are missed by methods that only quantify exon-exon junctions. Finally, we demonstrate that promoter-usage QTLs have distinct genetic architecture and are 50% more likely to be context-specific than alternatively spliced internal exons. In summary, we highlight how different RNA-seq quantification approaches capture distinct aspects of transcription and that characterizing the full spectrum of transcriptional consequences of genetic variation requires a combination of analytical strategies.

Introduction

Genome-wide association studies (GWAS) have discovered thousands of genetic loci associated with complex traits and diseases. However, identifying candidate causal genes and molecular mechanisms at these loci remains challenging. Complex trait-associated variants are enriched in regulatory elements and are therefore thought to act via regulation of gene expression levels, often in a cell type- and context-specific manner [1–3]. However, such variants are equally enriched among splicing quantitative trait loci (QTLs) [4] and incorporating splicing QTLs in a transcriptome-wide association study was found to increase the number of disease-associated genes by 2-fold [5]. Together with splicing, transcript sequence can also be altered by alternative promoter usage and polyadenylation, which we refer to collectively hereafter as transcript usage QTLs (tuQTLs). Alternative transcript start and end sites are estimated to underlie most transcript differences between human tissues [6,7] and alternative promoters are frequently deregulated in cancer [8]. Moreover, experimental procedures that specifically capture either 5' or 3' ends of transcripts have identified genetic variants that regulate promoter or 3' end usage [9,10]. However, computational methods to detect these changes in conventional RNA-seq data are still lacking. Consequently, their relative contribution to complex traits is currently unknown. Similarly, although a few studies have identified context-specific tuQTLs [11–13], none of them have specifically assessed the relative importance of distinct transcriptional mechanisms.

An established approach is to quantify the expression of full-length transcripts and use these estimates to infer changes at promoters and 3' ends [14]. A number of algorithms have been developed to estimate transcript expression levels from RNA-seq data [15,16]. However, a limitation of these approaches is that they can only quantify the expression of annotated transcripts. In the presence of unannotated transcripts, the accuracy of the transcript expression estimates can deteriorate rapidly [17]. This is a serious issue as 25-35% of the exon-exon junctions observed in RNA-seq data are not present in transcript databases [17], and up to 60% of the annotated transcripts are truncated at the 5' or 3' end (Figures S1 and S2). Incomplete reference transcriptome annotations are especially problematic when inferring the functional consequences of transcript usage QTLs, because missing annotations can lead to individual genetic changes being spuriously associated with multiple transcriptional events, for example, simultaneous changes in promoter usage and cassette exon inclusion (Fig. 1a, b).

To overcome the limitations of incomplete transcript annotations, multiple studies have quantified transcription at the level of individual exons [18,19] or exon-exon junctions (e.g. Altrans [17], Leafcutter [5], MAJIQ [20]). However, changes in exon expression are equally challenging to interpret because they could arise from differential gene expression, alternative splicing, or alternative promoter/3' end usage. Although quantifying exon-exon junction usage has the advantage of highlighting specific exons that are differentially regulated, junction-based approaches miss events that do not manifest at the level of junction reads. For example, Leafcutter is unable to detect retained introns or changes in 5' and 3' end usage [5]. Furthermore, it cannot differentiate alternative first exons, which are caused by promoter choice,

from other splicing events. Thus, exon-based and junction-based approaches are limited in their ability to interrogate various transcriptional mechanisms in detail.

Here, we first develop txrevise, a novel computational approach, implemented as an R package, to stratify transcript annotations into independent promoter, splicing and 3' end events. We then perform comprehensive mapping of gene expression and transcript usage QTLs in human macrophages exposed to three inflammatory (18 hours IFNɣ stimulation, 5 hours *Salmonella* infection and IFNɣ stimulation followed by *Salmonella* infection) and one metabolic stimulus (24 hours acetylated LDL (acLDL) stimulation), in up to 84 individuals. In these samples, we identify genetic effects at the level of total gene expression, transcript usage, alternative event usage and exon-exon junction usage. We find that promoter and 3' end usage QTLs constitute 55% of detected tuQTLs and exhibit genetic architectures that are distinct from canonical expression or splicing QTLs. Consequently, we find that colocalisations with many complex trait associations are missed when transcription is quantified only at the level of total gene expression or splice junction usage.

Results

Overview of the txrevise approach

To overcome the limitations of incomplete transcript annotations, we developed txrevise, a new computational method to stratify full-length transcripts into independent events. The key idea of txrevise is the use of shared exons between transcripts as a scaffold to construct independent transcriptional events that each represent individual alternative promoters, internal exons, and 3' ends (Fig. 1c). To make the construction of these events more efficient, we first extend truncated transcripts by copying over exons from the longest transcript of the gene (Figure S2). Second, to make the approach suitable for genes that contain non-overlapping transcripts, we also select a subset of transcripts that share the largest number of exons between them (Figure S3). Third, to ensure that the new alternative promoter and 3' end events do not capture splicing changes, we mask alternative exons that are not the first or last exons (Figure S4). Finally, we use Salmon [21] to estimate the relative expression of each alternative event. The R package as well as custom transcriptional events constructed by txrevise are available from GitHub (https://github.com/kauralasoo/txrevise).

We compared txrevise to three alternative approaches: (i) gene-level read count quantified with featureCounts [22], (ii) full-length transcript usage quantified with Salmon [21] (Fig. 1c), and (iii) exon-exon junction usage quantified with Leafcutter [5] (Fig. 1c). We found that for genes in the Ensembl database, the median count of alternative transcripts was eight, making their relative expression levels challenging to interpret, because the expression of each transcript has to be considered in the context of all other transcripts (Figure S5). In contrast, txrevise reduced the median count of alternative events to four while at the same time explicitly revealing the part of the gene that was affected by the tuQTL (Figure S5). A key advantage of txrevise over Leafcutter is that txrevise captures transcriptional events that do not manifest at the level of

junction reads, such as changes in 3' and 5' untranslated region (UTR) length and intron retention. Leafcutter, on the other hand, is able to discover novel exon-exon junctions and is thus well-suited for characterising rare or unannotated splicing events.

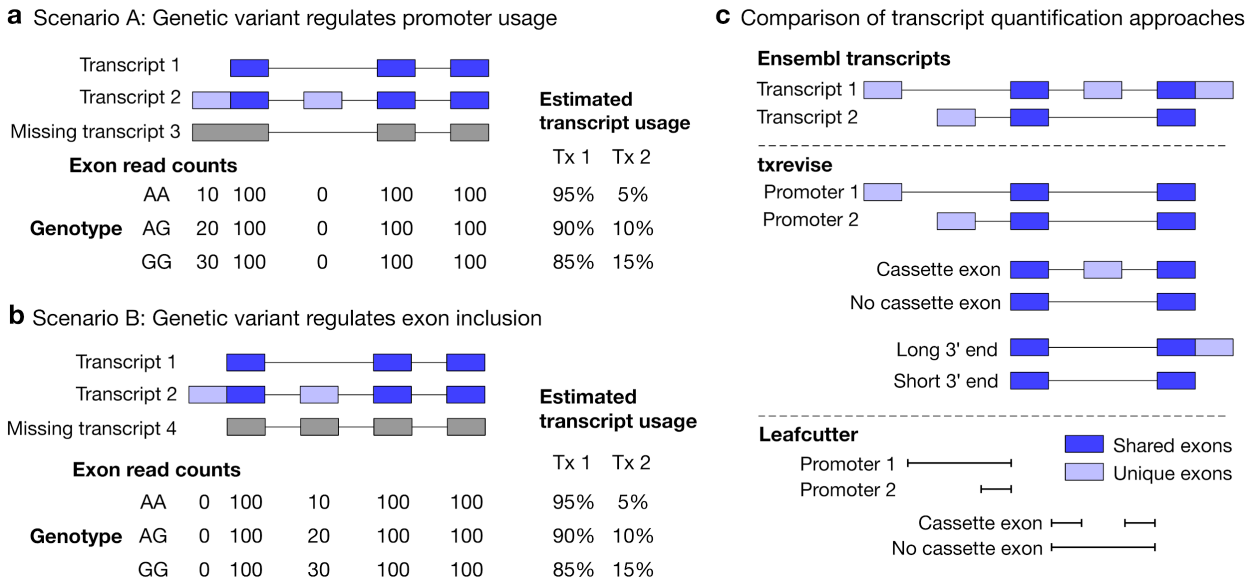

Fig. 1. Challenges of transcript usage quantification from RNA-seq data**.** Transcript quantification seeks to estimate the most likely configuration of *known* transcripts that best explains observed read counts supporting the inclusion of each exon. However, in the presence of unannotated transcripts, this can lead us to falsely conclude that a single genetic variant is associated with multiple transcriptional events. (**a**) In scenario A, each copy of the G allele increases the usage of transcript 3 by 10%. Since transcript 3 is missing from the annotation, reads originating from it are assigned to transcript 2. Thus, although the G allele only regulates promoter usage, we falsely conclude that it is also associated with increased inclusion of cassette exon present in transcript 2. (**b**) In scenario B, each copy of the G allele is associated with a 10% increase in the usage of transcript 4 containing alternative exon 2. Since transcript 4 is missing from the annotations, reads originating from it are assigned to transcript 2, leading us to wrongly conclude that the G allele is also associated with promoter usage. Note that scenarios A and B produce identical expression estimates for transcripts 1 and 2 although the underlying transcriptional change (promoter usage *vs* cassette exon inclusion) visible from exon read counts is different. Furthermore, in both scenarios, the effect of the genetic variant on transcript 2 is underestimated, because the reads assigned to transcript 2 are assumed to evenly spread across the promoter and the cassette exon. (**c**) Top panel: Two hypothetical transcripts that differ from each other at the promoter, at a cassette exon and at the 3' end. Middle panel: txrevise uses the exons shared between transcripts (dark blue) as a scaffold to construct three independent transcriptional events from the two original transcripts. Bottom panel: Leafcutter uses reads mapping to exon-exon junctions to identify alternatively excised introns.

Quantifying genetic effects on transcript usage

We applied all four analytical approaches discussed above to RNA-seq data from human induced pluripotent stem cell (iPSC)-derived macrophages exposed to three inflammatory stimuli (18 hours IFNɣ stimulation, 5 hours *Salmonella* infection, and IFNɣ stimulation followed by *Salmonella* infection) and one metabolic stimulus (24 hours acLDL stimulation). While the gene expression analysis of the IFNɣ + *Salmonella* dataset from 84 individuals has previously been described [3], the acLDL data from 70 individuals was newly generated for the current study. The acLDL dataset allowed us to assess how our results generalise to weaker non-inflammatory stimuli. Both datasets included unstimulated control samples (denoted 'naive' and 'Ctrl' in Fig. 2a).

Depending on the experimental condition and quantification method, we detected between 1500 and 3500 QTLs at the 10% false discovery rate (FDR) (Fig. 2a). Leafcutter consistently detected the lowest number of QTLs per condition, while txrevise detected approximately 30% more associations than other methods (Fig. 2a), 55% of which affected promoter or 3' end usage instead of internal exons (Figure S6). However, this increase in QTLs can be partially explained by the fact that txrevise detected multiple associations for ~24% of the genes while the full-length tuQTL analysis was limited to single lead association per gene (Figure S7). Some of these additional QTLs are likely to represent independent causal variants, such as the three independent tuQTLs detected for the IRF5 gene (Figure S8). Alternatively, these additional associations could also be caused by transcriptional coupling where promoter or 3' end choice directly influences the splicing of internal exons or *vice versa*.

Although multiple instances transcriptional coupling have been previously observed (reviewed in [23]), its genome-wide prevalence is still poorly understood. Proximal genetic variants predominantly regulate transcript usage in *cis*. Thus, a single causal variant associated with multiple transcriptional events could provide evidence for transcriptional coupling in the absence of full-length mRNA sequencing data [24]. To test this, we first focussed on the tuQTLs detected by full-length Ensembl transcripts. We compared the transcript with the smallest tuQTL p-value against the most highly expressed transcript. This revealed that 97% of the tuQTLs were seemingly associated with at least two transcriptional changes (e.g. alternative promoter and internal exon) and >50% were associated with all three transcriptional changes (different promoter, internal exons and 3' end) (see Methods). In contrast, a recent full-length mRNA sequencing experiment estimated coupling to occur between approximately 10% of the events [24], suggesting that our naive estimate is strongly inflated by the use of incomplete transcript annotations (Fig. 1a, b). To confirm this hypothesis, we turned to txrevise and Leafcutter analyses, where we detected multiple tuQTLs for only 24% and 10% of the genes, respectively (Figure S7). Furthermore, among the genes with multiple tuQTLs, 50% of the Leafcutter and 30% of the txrevise associations were caused by independent genetic variants ($R^2 < 0.2$), confirming that true transcriptional coupling seems to be rare (Figure S7). Moreover, the higher rate of coupling in the txrevise analysis can partly be explained by lowly expressed transcripts whose usage appears to increase when the expression of the dominant transcript decreases (Figure S9). Our results suggest that, although most genetic variants modulate individual

transcriptional events, high numbers of spurious associations between genotype and multiple transcriptional changes are detected when expression is quantified at the level of full-length transcripts.

Different quantification methods may be biased towards discovering events with specific genomic properties, which is not captured by the number of QTLs detected. To address this, we quantified how often were the lead QTL variants (FDR < 0.01) from different methods in high linkage disequilibrium (LD) (R^2 > 0.8) with each other (see Methods). Consistent with previous reports that tuQTLs are largely independent from eQTLs [4], we found that only 11-24% of the lead variants detected at the read count level replicated at the transcript level (R^2 > 0.8, irrespective of the replication p-value), independent of which quantification method was used (Fig. 2b). In contrast, ~50% of the Leafcutter QTLs were also detected by txrevise or full-length transcript usage approaches. Similarly, the tuQTLs detected by txrevise and full-length transcript usage quantification were in high LD more than 60% of the time (Fig. 2b). Finally, we found that while 44% of the txrevise internal exon QTLs were in high LD with Leafcutter QTLs, this decreased to ~20% for promoter and 3' end QTLs (Figure S6), confirming that Leafcutter is less well-suited to capture those events. Thus, different quantification approaches appear to be complementary, each one detecting slightly different sets of genetic associations.

Genomic properties of transcript usage QTLs

Next, to characterise the genetic associations detected by different quantification methods, we compared the relative enrichments of the identified QTLs across multiple genomic annotations. We constructed genomic tracks for eight annotations: open chromatin measured by ATAC-seq [3], promoter flanking regions (-2000 bp to +200 bp), 5' UTRs, coding sequence (CDS), introns, 3' UTRs, polyadenylation sites [25], and eCLIP binding sites for RNA binding proteins involved in splicing regulation (splice factors) [26]. We then used the hierarchical model implemented in fgwas [27] to estimate the enrichment of each genomic annotation among the QTLs detected by each quantification method. Consistent with the limited overlap between eQTLs and tuQTLs (Fig. 2b), we found that eQTLs were strongly enriched in sites of open chromatin (Fig. 2c; log enrichment of 3.31, 95% CI [3.15, 3.47]), whereas all transcript-level QTLs were enriched at the binding sites of splicing factors detected by eCLIP (Fig. 2c, mean log enrichment of 2.29). Importantly, when all txrevise tuQTLs were pooled, the enrichment patterns were broadly similar to tuQTLs detected by full-length Ensembl transcripts (Fig. 2c). This suggests that txrevise events and full-length transcripts capture similar genetic associations but txrevise facilitates more accurate identification of the underlying transcriptional event (i.e. promoter, internal exon or 3' end usage) (Fig. 2b). Finally, compared to Leafcutter, full-length transcript usage and txrevise QTLs were both more strongly enriched at 3' UTRs (Fig 2c, mean log enrichment of 1.85), suggesting that they might capture changes in 3' UTR length that do not manifest at the level of junction reads and are thus missed by Leafcutter.

If the coupling between promoter usage, splicing and 3' end choice is as rare as suggested by txrevise, then this should be reflected by the genomic features that the associated variants are enriched in. Conversely, pervasive coupling between distinct transcriptional mechanisms would

predict that the associated variants would share most of their genomic properties. To assess this, we repeated the fgwas analysis on the promoter, internal exon and 3' end QTLs detected by txrevise as well as Leafcutter splicing QTLs. We found that Leafcutter and internal exon QTLs showed broadly similar enrichment patterns, with a strong enrichment at the binding sites of splice factors (Fig. 2d, mean log enrichment of 2.53). In contrast, promoter and 3' end usage QTLs were specifically enriched at promoters (Fig. 2d; log enrichment of 2.76, 95% CI [2.59, 2.95]) and 3' UTRs (Fig 2d; log enrichment of 3.60, 95% CI [3.43, 3.76]), respectively (Fig. 2d), and showed only a modest enrichment at splice factor binding sites (Fig. 2d; mean log enrichment of 1.17). Compared to other events, promoter usage QTLs were relatively more enriched in open chromatin regions (log enrichment of 1.58, 95% CI [1.42, 1.74]) and were also 65% more likely to overlap chromatin accessibility QTLs in macrophages [3] ($R^2 > 0.9$) (Fisher's exact test p-value = 3.87×10^{-5}). Thus, promoter usage, splicing and 3' end usage appear to be regulated by largely independent sets of genetic variants enriched in distinct genomic regions.

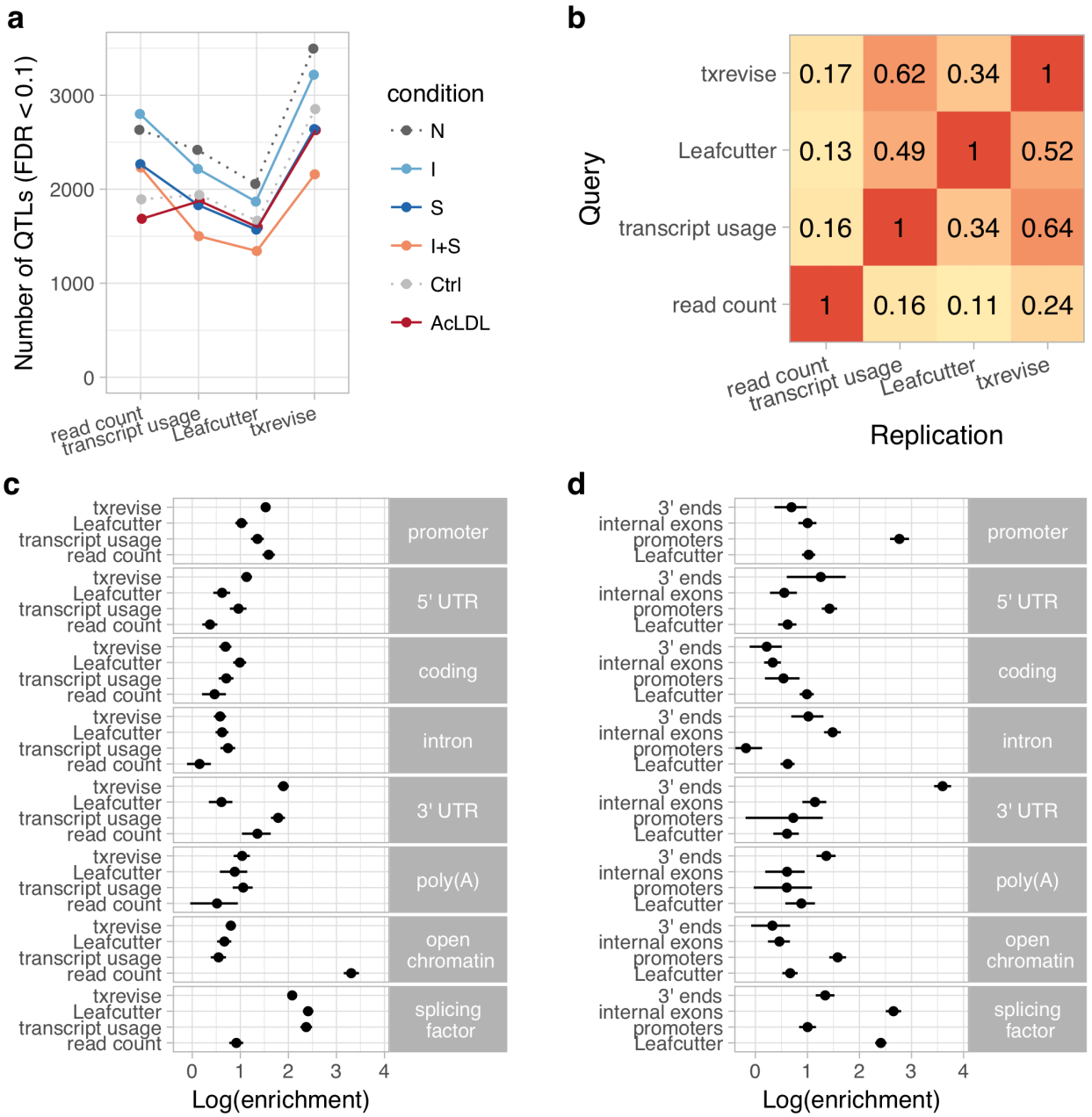

Fig. 2 Diversity of QTLs detected by different quantification methods. In panels a-c, all txrevise QTLs from promoters, internal exons and 3' ends have been pooled to facilitate comparison with eQTLs as well as Leafcutter and full-length transcript usage QTLs. (**a**) Number of QTLs detected by read count, full-length transcript usage, Leafcutter and txrevise methods in each condition. (**b**) Sharing of QTLs detected by four quantification methods. The numbers on the heatmap show the fraction of QTLs detect by one method that were replicated by the three other methods (R^2 > 0.8 between lead variants). Only QTLs with FDR < 0.01 were included in the analysis. (**c**) Enrichment of genomic annotations at QTLs detected by the four quantification methods. (**d**) Comparison of Leafcutter tuQTLs to promoter, internal exon and 3' end usage QTLs detected by txevise. Genomic annotations used for enrichment analysis: *promoter* - promoter flanking regions (-2000 bp to +200 bp); *5' UTR, coding, intron, 3' UTR* - corresponding

regions extracted from Ensembl transcripts; *poly(A)* - experimentally determined polyadenylation sites (+/- 25 bp) [25]; *open chromatin* - open chromatin regions from macrophages [3]; *splicing factor* - experimentally determined binding sites of splicing factors detected by eCLIP [26]. Panels c and d show the natural logarithm of enrichment for each annotation.

Colocalisation with complex trait associations

To assess the relevance of different QTLs for interpreting complex trait associations, we performed statistical colocalisation analysis with GWAS summary statistics for 33 immune-mediated and metabolic traits and diseases (see Methods). We found that 47 of 138 colocalised QTLs influenced total gene expression level (Fig. 3a). In contrast, the remaining 91 colocalised QTLs were associated with at least one of the transcript-level phenotypes (full-length transcript usage, txrevise or Leafcutter) but not with total gene expression (Fig. 3a). Similarly, 40/91 transcript-level colocalisations were detected only by a single transcript quantification approach (Fig. 3a). An important caveat of this analysis is that it does not directly test if the colocalisations are specific to one quantification method or simply missed by others because of limited power. Thus, our estimates of method-specificity are likely to be inflated.

Finally, to quantify the relative contribution of promoter usage, splicing and 3' end usage to complex traits, we stratified the txrevise colocalisation by transcriptional event type. We found that 42 of 80 colocalised QTLs influenced internal exons and the rest regulated promoters and 3' ends (Fig. 3b). We were able to replicate known associations between splicing of exon 2 in *CD33* and Alzheimer's disease (Figure S10) [28] and splicing of exon 13 in *HMGCR* and LDL cholesterol (Figure S11) [29]. Importantly, while half of the promoter and internal exon colocalisations were also detected by Leafcutter, none of the 3' end events were captured by Leafcutter, probably because these are less likely to manifest at the level of junction reads (Fig. 3b).

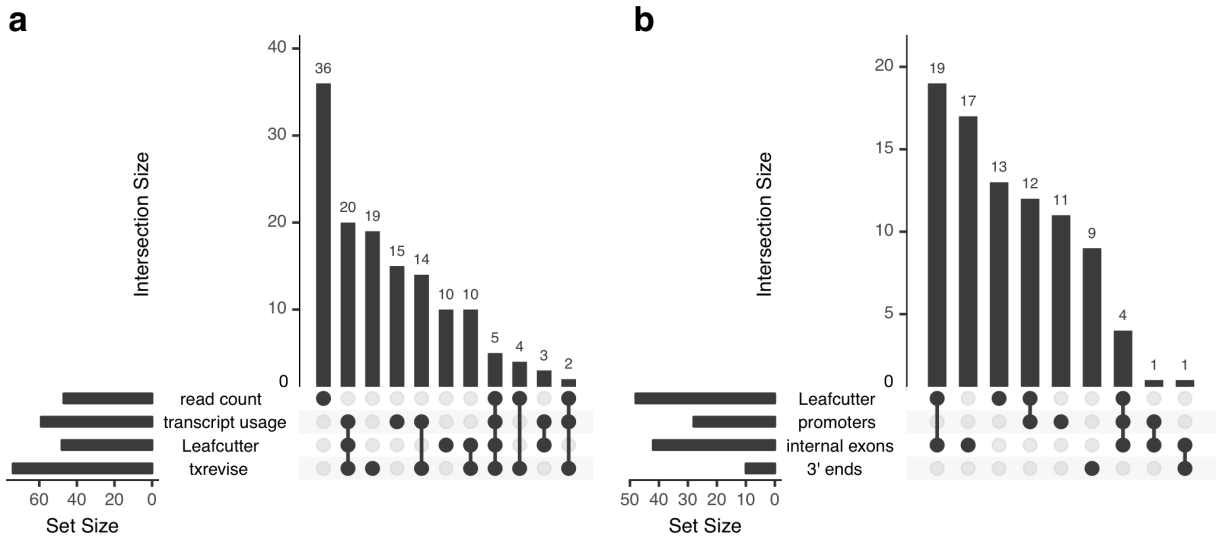

Fig. 3. Colocalisation between GWAS hits for 33 complex traits and QTLs. (**a**) Sharing of colocalisations between the four quantification methods. The UpSetR plot shows the total number of colocalised trait-gene pairs detected by different quantification methods (horizontal bars) and overlap between different methods (vertical bars). (**b**) Sharing of colocalisations between Leafcutter and different txrevise event types. The UpSetR plot shows the total number of colocalised trait-gene pairs detected by different quantification methods (horizontal bars) and overlap between different methods (vertical bars).

Condition-specificity of genetic associations

Next, we explored how the genetic effects of eQTLs and tuQTLs varied in response to stimuli. To define response QTLs, we started with QTLs detected (FDR < 10%) in each of the four simulated conditions (I, S, I+S and acLDL) and used an interaction test to identify cases where the QTL effect size was significantly different between the simulated and corresponding naive condition (FDR < 10%). To exclude small but significant differences in effect size, we used a linear mixed model to identify QTLs where the interaction term explained more than 50% of the total genetic variance in the data (see Methods). Although the fraction of QTLs that were response QTLs varied greatly between conditions (Fig. 4a) and correlated with the number of differentially expressed genes (Figure S12) as previously reported [1], we found that the fraction of response tuQTLs was relatively consistent between the four quantification methods (Fig. 4a). While previous reports have highlighted that eQTLs are more condition-specific than tuQTLs [11], we found no clear pattern in our data with stronger stimuli (S and I+S) showing larger fraction of condition-specific eQTLs, and weaker stimuli (I, acLDL) showing smaller fraction of response eQTLs (Fig. 4a) compared to tuQTLs. However, when we focussed on the transcriptional events detected by txrevise, we found that promoter usage QTLs were 50% more likely to be response QTLs than tuQTLs regulating either internal exons or 3' ends (Fig. 4b) (Fisher's exact test combined p-value = 2.79×10^{-6}).

Finally, we assessed the condition-specificity of QTLs that colocalised with complex trait loci. We found that, on average, 12% of the GWAS colocalisations corresponded to response QTLs (Fig. 4c). One such example is an IFNɣ-specific promoter usage QTL for the *CD40* gene that colocalises with a GWAS signal for rheumatoid arthritis [30]. The alternative C allele of the rs4239702 variant is associated with increased usage of the transcript with the short 5' UTR (Fig. 4e, f). This tuQTL was also visible at the absolute expression level of the two alternative promoters (Figure S13), but was missed by Leafcutter, because there is no change in junction reads. Although the variant was not significantly associated with total gene expression level (Figure S13), the two promoters contain the same start codon. As a result, the likely functional consequence of the *CD40* tuQTL is modulation of protein abundance. Although the same tuQTL was also detected at the full-length transcript usage level, the affected transcripts also differ from each other by alternatively spliced exon 6, making it challenging to interpret the result (Fig. 4e). Finally, the preferential upregulation of the transcript with the short 5' UTR after inflammatory stimulus is also supported by FANTOM5 capped analysis of gene expression (CAGE) data from primary macrophages (Figure S14) [31].

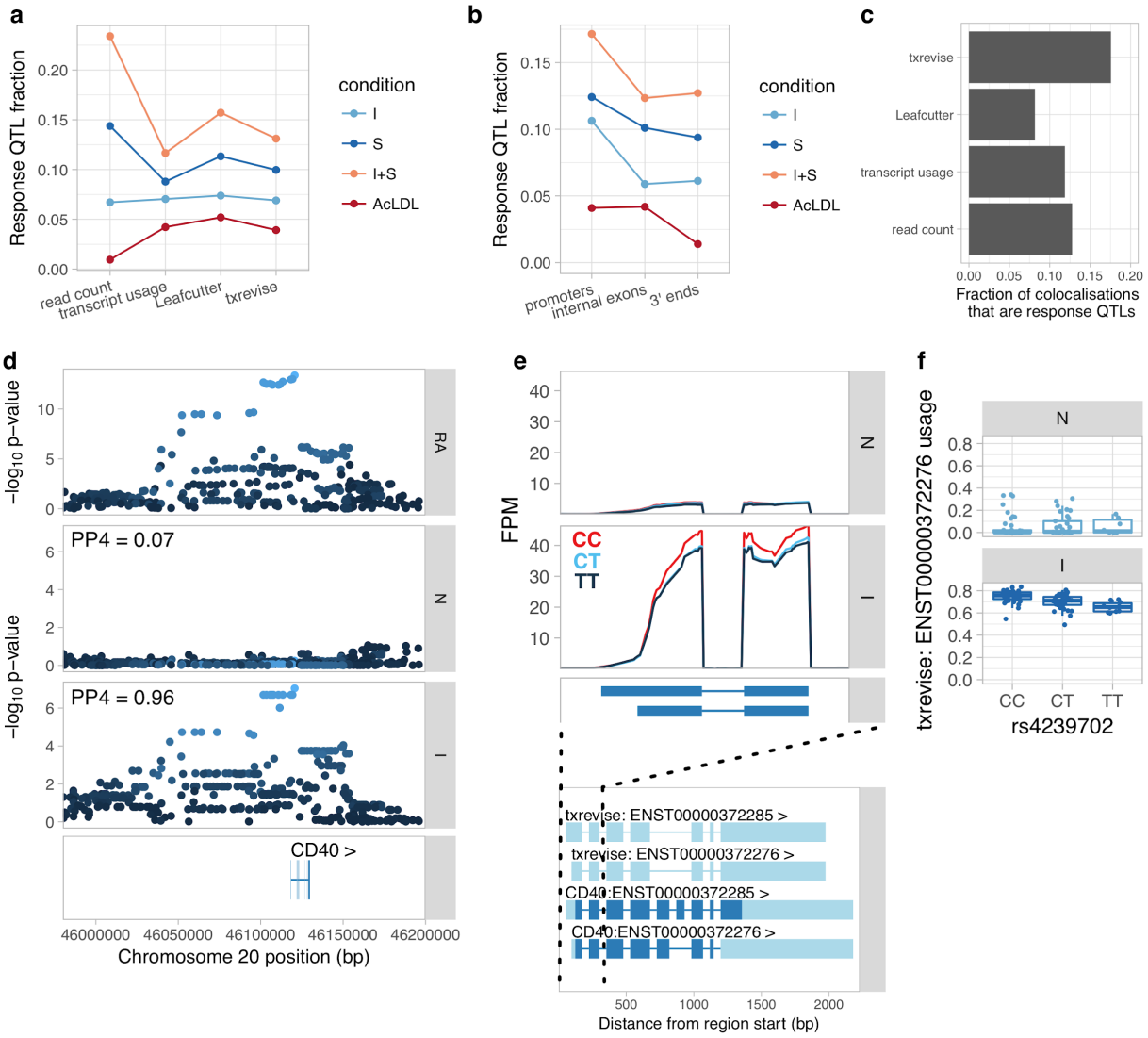

Fig. 4 Condition-specificity of eQTLs and tuQTLs. (**a**) Fraction of all QTLs detected in each simulated condition that are response QTLs (FDR < 10% and more than 50% of the genetic variance explained by the interaction term). (**b**) Fraction of txrevise tuQTLs classified as response QTLs, stratified by the part of the gene that they influence (promoters, internal exons or 3' ends). (**c**) Fraction of GWAS colocalisations that are response QTLs. (**d**) Colocalisation between a GWAS hit for rheumatoid arthritis (RA) and IFNɣ-specific tuQTL at the *CD40* locus. PP4 represents the posterior probability from coloc [32] that the GWAS and QTL signals share a single causal variant. (**e**) Top panel: The lead GWAS variant (rs4239702) is associated with increased expression of the short 5' UTR of the CD40 gene. Bottom panel: Ensembl annotations couple the short 5' UTR to skipped exon 6, but this is not supported by RNA-seq data (Figure S13). (**f**) Relative expression of the short 5' UTR stratified by the genotype of the lead GWAS variant.

Discussion

We have performed a comprehensive analysis of the genetic determinants of transcript usage in human iPSC-derived macrophages exposed to four different stimuli. Our simple approach to stratify transcripts into individual events greatly improved the interpretability of molecular mechanisms underlying tuQTLs. Consequently, we were able to discover that 55% of the transcript-level associations affected promoter or 3' end usage and these variants were enriched in markedly different genomic features relative to canonical splicing QTLs. We also found that promoter usage QTLs were 50% more likely to be condition-specific than other transcriptional events. These analyses would not have been feasible using full-length transcripts due to the high number of false positives (Fig 1a, b), and many of these associations were also missed by Leafcutter because they did not manifest at the level of junction reads. Event-level analysis might suffer from loss of power when multiple transcriptional events are coupled at the transcript level. However, both our results as well as a recent full-length mRNA sequencing study [24] suggest that such coupling is relatively rare, affecting ~10% of the transcriptional events. A caveat of our analysis is that txrevise is likely to miss coupling between nearby exons, because they would be part of the same transcriptional event. Nevertheless, event-level analysis allowed us to often detect multiple independent tuQTLs per gene that were missed by the transcript-level quantification.

Our approach is related to, and inspired by, the alternative event annotations used in MISO [33]. However, the alternative promoter and 3' UTR annotations in MISO have not been updated in the past 10 years and no computer code is provided to generate them. In addition, txrevise constructs much longer transcriptional events than the individual alternative exons considered by MISO. Finally, txrevise also explicitly handles truncated transcripts while MISO assumes those to be the true transcripts. A promising new alternative is Whippet, which quantifies transcriptional events by aligning reads directly to the splice graph of the gene [34].

An important limitation of txrevise is that it is only able to quantify splicing events present in reference transcript databases. However, our approach can easily be extended by incorporating additional annotations such experimentally determined promoters from the FANTOM5 [35] projects or alternative polyadenylation sites from the PolyAsite database [25]. Another powerful alternative might be to incorporate novel transcripts identified by transcript assembly methods such as StringTie [36] into existing annotation databases. Nevertheless, since txrevise relies on Salmon for event-level quantification, it is still susceptible to some of the same limitations as full-length transcript quantification. Even though event-level analysis reduces the problem a bit, a positive transcript expression estimate does not guarantee that any specific exon is actually present in the transcript, especially if the transcript annotations are inaccurate (Fig. 1b). Secondly, transcript quantification is susceptible to a type of false positive whereby transcripts with background expression level appear to be downregulated when total expression of the gene increases (Figure S9). Therefore, it is important to visually confirm candidate transcriptional events using either a genome browser or tools such as wiggleplotr [37] before embarking on follow-up experiments.

A key aim of QTL mapping studies is to elucidate the molecular mechanisms underlying complex trait associations. In our analysis, we found that over 50% of the genetic effects that colocalise with complex traits regulated transcript usage and did not manifest at the total gene expression level. Moreover, 48% of the transcript-level colocalisations affected promoter or 3' end usage instead of splicing of internal exons. Finally, no single quantification method was able to capture the full range of genetic effects, confirming that different quantification approaches often identify complementary sets of QTLs [17,38]. Consequently, there is great potential to discover additional disease associations by re-analysing large published RNA-seq datasets such as GTEx [39] with state-of-the-art quantification methods.

Methods

Cell culture and reagents

Donors and cell lines

Human induced pluripotent stem cells (iPSCs) from 123 healthy donors (72 female and 51 male) (Table S1) were obtained from the HipSci project [40]. Of these lines, 57 were initially grown in feeder-dependent medium and 66 were grown in feeder-free E8 medium. The cell lines were screened for mycoplasma by the HipSci project [40]. All samples for the HipSci resource were collected from consented research volunteers recruited from the NIHR Cambridge BioResource (http://www.cambridgebioresource.org.uk). Samples were collected initially under ethics for iPSC derivation (REC Ref: 09/H0304/77, V2 04/01/2013), with later samples collected under a revised consent (REC Ref: 09/H0304/77, V3 15/03/2013).

The details of the iPSC culture, macrophage differentiation and stimulation for the IFNɣ + *Salmonella* study have been described previously [3] (Table S2). Macrophages for the acLDL study were obtained from the same differentiation experiments described above.

AcLDL stimulation

Macrophages differentiated from a total of 71 iPSC lines were used for the acLDL stimulation. Macrophages were grown in RPMI 1640 (Gibco) supplemented with 10% FBS (labtech), 2 mM L-glutamine (Sigma) and 100 ng/ml hM-CSF (R&D) at a cell density of 150,000 cells per well on a 6-well plate. On day 6 of the macrophage differentiation, two wells of the 6-well plate were exposed to 100 µg/ml human acLDL (Life Technologies) for 24 hours, whereas the other two wells were incubated in fresh RPMI 1640 medium without stimulation throughout this period.

For RNA extraction, cells were washed once with PBS and lysed in 300 µl of RLT buffer (Qiagen) per well of a 6-well plate. Lysates from two wells were immediately pooled and stored at -80°C. RNA was extracted using a RNA Mini Kit (Qiagen) following the manufacturer's instructions and eluted in 35 µl nuclease-free water. RNA concentration was measured using

NanoDrop, and RNA integrity was measured on Agilent 2100 Bioanalyzer using a RNA 6000 Nano Total RNA Kit.

RNA sequencing and quality control

All RNA-seq libraries from the acLDL study were constructed manually using poly-A selection and the Illumina TruSeq stranded library preparation kit. The TruSeq libraries were quantified using Bioanalyzer and manually pooled for sequencing. The samples were sequenced on Illumina HiSeq 2000 using V4 chemistry and multiplexed at 6 samples/lane. The control and acLDL stimulated RNA samples from a single donor were always sequenced in the same experimental batch. Sample metadata is presented in Table S3. RNA-seq reads were aligned to the GRCh38 reference genome and Ensembl 87 transcript annotations using STAR v2.4.0j [41]. Subsequently, VerifyBamID v1.1.2 [42] was used to detect and correct any sample swaps between donors. Two samples from one donor (HPSI0513i-xegx_2) were excluded from downstream analysis, because they appeared to be outliers on the principal component analysis (PCA) plot of the samples.

Quantifying gene and transcript expression

We used four alternative strategies to quantify transcription from RNA-seq data: (i) gene-level read count quantified with featureCounts [22], (ii) full-length transcript usage quantified with Salmon [21] (Fig. 1c), (iii) usage of transcriptional events quantified with txrevise, and (iv) exon-exon junction usage quantified with Leafcutter [5].

Gene-level read count

We used featureCounts v1.5.0 [22] to count the number of uniquely mapping fragments overlapping transcript annotations from Ensembl 87. We excluded short RNAs and pseudogenes from the analysis leaving 35,033 unique genes of which 19,796 were protein coding. Furthermore, in both IFNɣ + *Salmonella and* acLDL dataset we used only genes with mean expression in at least one of the conditions greater than 1 transcripts per million (TPM) [43] in all downstream analyses. This resulted in 12,660 and 12,103 genes included for analysis in the IFNɣ + *Salmonella and* acLDL datasets, respectively. We quantile-normalised the data and corrected for sample-specific GC content bias using the conditional quantile normalisation (cqn) [44] R package as recommended previously [45].

Full-length transcript usage

We downloaded the FASTA files with messenger RNA (mRNA) and non-coding RNA sequences from the Ensembl website (version 87). We concatenated the two files and used salmon v0.8.2 [21] with '--seqBias --gcBias --libType' options to quantify the expression level of each transcript. We used tximport [46] package to import the expression estimates into R and calculated the relative expression of each transcript by dividing the TPM expression estimate of each transcript with the sum of the expression estimates of all transcripts of the gene. We found that this approach gave rise to a type of false positive where transcripts with background

expression level appeared to be downregulated as the expression of the dominant transcript increased (Figure S9). This was likely caused by the fact that the estimated expression level of a transcript in TPM units was almost never exactly zero.

Quantifying transcriptional events with txrevise

We downloaded exon coordinates for all Ensembl 87 transcripts using the `makeTxDbFromBiomart` function from the GenomicFeatures [47] R package. We also downloaded metadata for these transcripts using the biomart [48] R package. Finally, we extracted transcript tags from the GTF file downloaded from the Ensembl website. This step was necessary, because Ensembl contains a large number of truncated transcripts (marked with cds_start_NF or cds_end_NF tags) (Figure S1), but this information is not present in biomart.

We developed the txrevise R package to pre-process transcript annotations prior to quantification. First, we extended all truncated protein coding transcripts using exons from the longest annotated transcript of the gene that was part of the GENCODE Basic gene set (Figure S2). We also performed the same step on transcripts annotated in Ensembl as `retained_intron`, `processed_transcript` or `nonsense_mediated_decay`, because they often ended abruptly in the middle of the introns and were unlikely to correspond to true transcription start and end sites.

Next, we focused on splitting full-length transcripts into alternative promoters, internal exons and 3' ends. However, some genes contained either non-overlapping transcripts or very short transcripts that complicated this process. Thus, for each gene we first identified a subset of transcripts that shared the largest number of exons with each other. We then used the shared exons as a scaffold and constructed sets of independent promoters, internal exons and 3' ends (group 1) (Figure S3). We repeated this process for a second subset of transcripts that shared the most exons with each other (group 2) (Figure S3). Thus, the original transcripts from each gene were split into up to six sets of transcriptional events (two groups of alternative promoters, internal exons and 3' ends). Next, to ensure that the new alternative promoter and 3' end events did not capture splicing changes, we masked all alternative exons that were not the first or last exons (Figure S4). This final step can optionally be skipped to discover more association at the expense of losing some interpretability, because a subset of the promoter and 3' end events might be tagging splicing changes. We used Salmon [21] to independently quantify the expression of each set of transcriptional events. Finally, we used tximport [46] to import the expression estimates into R and calculated the relative expression of each transcriptional event by dividing the TPM expression estimate of each event with the sum of the expression estimates of all events in one group.

Quantifying intron excision ratios with Leafcutter

Finally, we used Leafcutter [5] to quantify the relative excision frequencies of alternative introns. We used the spliced alignments from STAR as input to Leafcutter. We did not correct for reference mapping bias, because we wanted to be able to directly compare Leafcutter results

with those from Salmon and there is no obvious way to correct for reference mapping bias in Salmon quantification. We used the default parameters of requiring at least 50 reads supporting each intron cluster and allowing introns of up to 500kb in length.

Mapping expression and transcript usage QTLs

Preparing genotype data

We obtained imputed genotypes for all of the samples from the HipSci [40] project. We used CrossMap v0.1.8 [49] to convert variant coordinates from GRCh37 reference genome to GRCh38. Subsequently, we filtered the VCF file with bcftools v.1.2 to retain only bi-allelic variants (both SNPs and indels) with IMP2 score > 0.4 and minor allele frequency (MAF) > 0.05. We created a separate VCF files for the IFNɣ + *Salmonella* study (84 individuals) and the acLDL study (70 individuals). The same VCF files were used for all downstream analyses and were imported into R using the SNPRelate [50] R package.

Association testing

We used QTLTools [51] to map QTLs in two stages. First, we used the permutation pass with ‘--permute 10000 --grp-best’ options to calculate the minimal lead variant p-value for each feature (gene, transcript or splicing event) in a +/- 100 kb window around each feature. The ‘--grp-best’ option ensured that in case of transcript usage QTLs, the permutation p-values were corrected for the number of alternative transcripts, exon-exon junction or transcriptional events tested. Secondly, we used the nominal pass to calculate nominal association p-values in a +/- 500 kb *cis* window around each feature. We used a larger *cis* window for the nominal pass to ensure that we did not have missing data in the colocalisation analysis (see below), where we used the +/- 200 kb *cis* window around each lead QTL variant.

QTL replication between quantification methods

To compare the QTLs detected by different quantification methods, we estimated the fraction of QTL lead variants detected by each method that were replicated by the other methods. Since read count and full-length transcript usage analysis were performed at the gene level, we decided to perform the replication analysis at the gene level as well. Because txrevise and leafcutter quantified multiple events per gene and sometimes detected multiple independent QTLs (Figure S7), we picked the lead variant with the smallest p-value across all of the events quantified for a given gene as the gene-level lead variant. For each pairwise comparison of quantification methods, we first identified all lead variant-gene pairs with FDR < 0.01 detected by the query method. Subsequently, we extracted the lead variants for the same genes detected by the replication method and estimated the fraction of those that were in high LD (R^2 < 0.8) with each other. We then repeated this analysis for all pairs of quantification methods. Note that this measure is not necessarily symmetric between the quantification methods and also depends on the statistical power of each method. Since Leafcutter was less powered than other methods, it also replicated smaller fraction of QTLs detected by the other methods. In contrast, 50% of the Leafcutter QTLs were replicated by txrevise and full-length transcript usage.

QTL enrichment in genomics annotations

Constructing genomic annotations

Gene features. We downloaded transcript annotations from Ensembl version 87 [52] using the GenomicFeatures [47] R package. We retained only protein coding transcripts and used `fiveUTRsByTranscript`, `threeUTRsByTranscript`, `cdsBy`, `intronsByTranscript` and `promoters` functions to extract 5' UTRs, 3' UTRs, coding sequences, introns and promoters, respectively. We defined promoters as sequences 2000 bp upstream and 200 bp downstream of the annotated transcription start sites.

Polyadenylation sites. We downloaded the coordinates of experimentally determined human polyadenylation sites from the PolyASite database (version r1.0) [25]. After converting the coordinates to the GRCh38 reference genome with CrossMap [49], we extended each polyadenylation site to +/-25 bp from the center of the site.

Chromatin accessibility. We downloaded the coordinates of accessible chromatin regions in macrophages across four conditions (N, I, S, I + S) from our previous study [3]. Specifically, we downloaded the ATAC_peak_metadata.txt.gz file from Zenodo (https://doi.org/10.5281/zenodo.1170560).

RNA binding proteins. We downloaded processed eCLIP [53] peak calls for 93 RNA binding proteins (RBPs) [26] from the ENCODE web site (https://www.encodeproject.org). Each protein was measured in two biological replicates, resulting in 186 sets of peaks. We only used data from the K562 myelogenous leukemia cell line. We further used Supplementary Table 1 from [26] to identify a subset of 29 RBPs that have previously been implicated in splicing regulation, five factors that have been implicated in 3' end processing and two factors (SRSF7 and HNRNPK) that have been implicated in both. Within each group (splicing, 3' end processing and both), we first removed all peaks that were detected only once and then merged all peaks into a single genomic annotation.

Enrichment analysis

We used fgwas v0.3.6 [27] with the '-fine' option to identify the genomic annotations in which different types of QTLs were enriched. We converted QTLtools p-values to z-scores using the `stats.norm.ppf(p/2, loc=0, scale=1)` function from SciPy [54], where p is the p-value from QTLtools. The sign of the z-score was determined based on the sign of the QTL effect size. We included all genomic annotations into a joint fgwas model using the '-w' option. For the enrichment analysis we used QTLs from the naive condition only, but we found that the enrichments patterns were very similar in all stimulated conditions.

Overlap with genome-wide association studies

Summary statistics

We obtained full summary statistics for ten immune-mediated disorders: inflammatory bowel disease (IBD) including ulcerative colitis (UC) and Crohn's disease (CD) [55], Alzheimer's disease (AD) [56], rheumatoid arthritis (RA) [30], systemic lupus erythematosus (SLE) [57], type 1 diabetes (T1D) [58], schizophrenia (SCZ) [59], multiple sclerosis (MS) [60], celiac disease (CEL) [61] and narcolepsy (NAR) [62]. We also obtained summary statistics for type 2 diabetes (T2D) [63], cardiovascular disease (CAD) [64,65] and myocardial infarction (MI) [64]. Finally, we obtained summary statistics for 20 cardiometabolic traits from a recent meta-analysis [66]. Summary statistics for T1D, CEL, IBD, RA, AD, MS and SLE were downloaded in 2015. SCZ, T2D and NAR were downloaded in 2016. T2D summary statistics were converted from GRCh36 to GRCh37 coordinates using the LiftOver tool, all of the other summary statistics already used GRCh37 coordinates.

Colocalisation analysis

We used coloc v2.3-1 [32] to test for colocalisation between gene expression and transcript usage QTLs and GWAS hits. We ran coloc on a 400 kb region centered on each lead eQTL and tuQTL variant that was less than 100kb away from at least one GWAS variant with a nominal p-value < 10^{-5}. We used the following prior probabilities: p1 = 10^{-4}, p2 = 10^{-4} and p12 = 10^{-5}. We then applied a set of filtering steps to identify a stringent set of eQTLs and tuQTLs that colocalised with GWAS hits. Similarly to a previous study [67], we first removed all cases where PP3 + PP4 < 0.8, to exclude loci where we were underpowered to detect colocalisation. We then required PP4/(PP3+PP4) > 0.9 to only keep loci where coloc strongly preferred the model of a single shared causal variant driving both association signals over a model of two distinct causal variants. We excluded all colocalisation results from the MHC region (GRCh38: 6:28,510,120-33,480,577) because they were likely to be false positives due to complicated LD patterns in this region. We only kept results where the minimal GWAS p-value was < 10^{-6}. Plots illustrating the sharing of colocalised GWAS signals by different quantification methods were made using UpSetR [68].

Code availability

The Snakemake [69] files used for gene and transcript expression quantification, QTL mapping and colocalisaton are available from the project's GitHub repository (https://github.com/kauralasoo/macrophage-tuQTLs). The same repository also contains R scripts that were used for all data analysis and figures. The txrevise R package is available from GitHub (https://github.com/kauralasoo/txrevise) and wiggleplotr R package that was used to make transcript read coverage plots is available from Bioconductor (http://bioconductor.org/packages/wiggleplotr/).

Data availability

RNA-seq data from the acLDL stimulation study is available from ENA (ERP022909) and EGA (EGAS00001000876). RNA-seq data from the IFNɣ + *Salmonella* study is available from ENA (ERP020977) and EGA (EGAS00001002236). The imputed genotype data for HipSci cell lines is available from ENA (ERP013161) and EGA (EGAD00010000773). Processed data and QTL summary statistics are available from Zenodo: https://zenodo.org/communities/macrophage-tuqtls/.

Acknowledgements

We thank Jeremy Schwartzentruber for his helpful comments on the manuscript. We thank WTSI DNA Pipelines and Cytometry Core Facility for their sequencing and flow cytometry services. We thank Elena Vigorito and Joanna M.M Howson (Cardiovascular Epidemiology Unit) for their help with statistical analyses during the early phases of this project. This work was supported by the Wellcome Trust (WT098051) and the British Heart Foundation Cambridge Centre of Excellence (RE/13/6/30180). K.A. was supported by a PhD fellowship from the Wellcome Trust (WT099754/Z/12/Z) and a postdoctoral fellowship from the Estonian Research Council (MOBJD67). The Cardiovascular Epidemiology Unit is supported by the UK Medical Research Council (MR/L003120/1), British Heart Foundation (RG/13/13/30194) and NIHR Cambridge Biomedical Research Centre. The iPSC lines were generated at the Wellcome Sanger Institute, under the Human Induced Pluripotent Stem Cell Initiative funded by a strategic award (WT098503) from the Wellcome Trust and Medical Research Council. We also acknowledge Life Science Technologies Corporation as the provider of cytotune.

Author contributions

K.A., D.S.P. and D.J.G. wrote the paper with input from all authors. K.A. and J.R. performed the macrophage differentiation experiments. J.R. optimised and performed the acLDL stimulation experiments. K.A. analysed the data. K.A., D.S.P., D.F.F. and D.J.G. designed the experiments. D.S.P., D.J.G. and J.D. supervised the research.

Disclosures

Since October 2015, Daniel Freitag has been a full time employee of Bayer AG, Germany.

Supplementary Figures

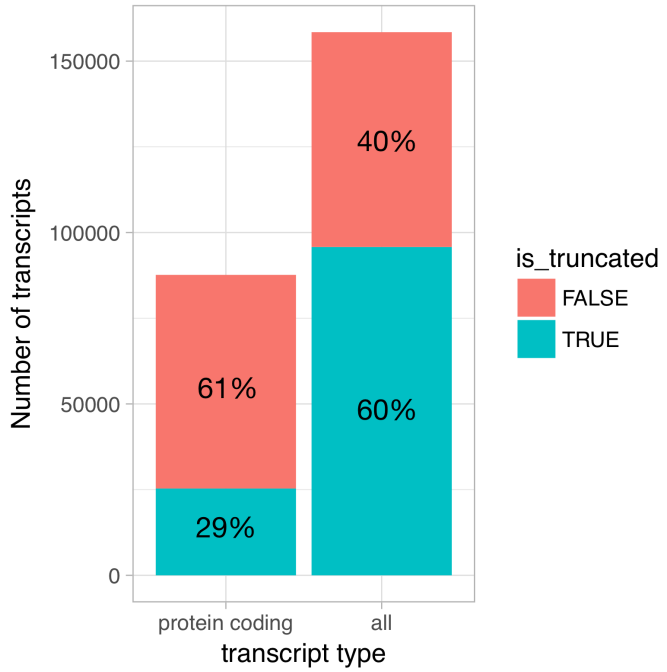

Figure S1 Truncated transcripts in the Ensembl database. For protein coding transcripts, we extracted the `cds_start_NF` and `cds_end_NF` fields from the Ensembl v87 GTF file to identify transcripts that were truncated at either 5' or 3' ends. For non-protein coding transcripts, we considered all transcripts annotated as `nonsense_mediated_decay`, `processed_transcript` or `retained_intron` to be truncated at both 5' or 3' ends, because we observed that many of those started and ended abruptly in the middle of exons. We included only protein coding genes in the analysis.

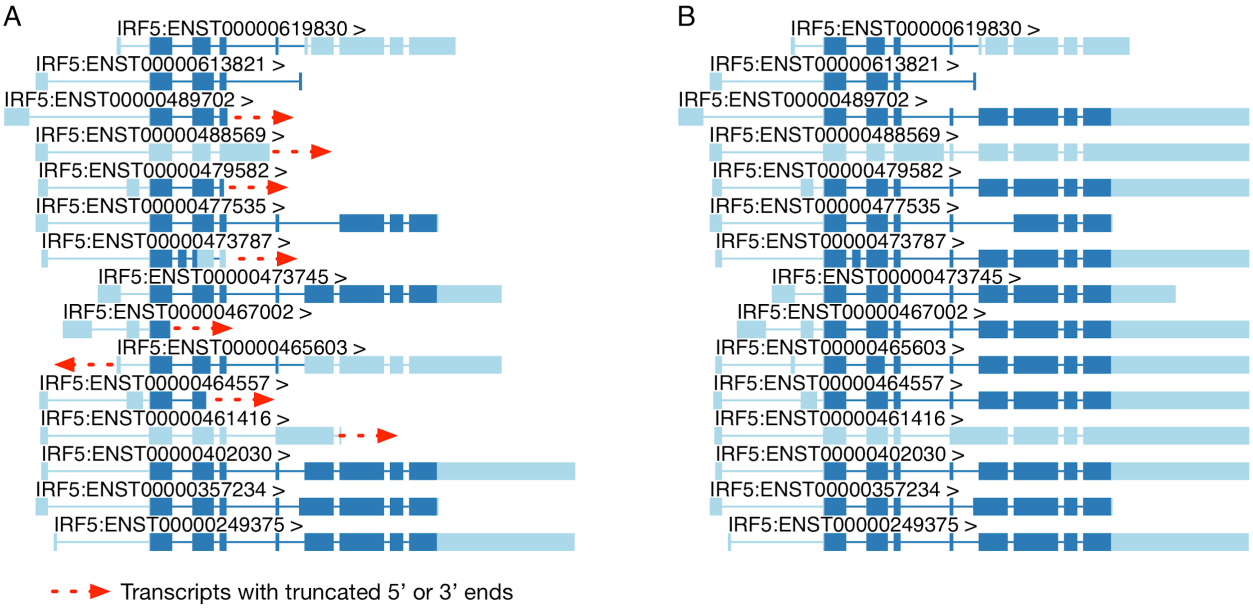

Figure S2 Extending truncated transcript annotations**.** (**A**) Original transcript annotations for IRF5. (**B**) Truncated IRF5 transcripts have been extended by copying over exons from the longest transcript of the gene (ENST00000402030).

Group 1: 14 transcripts share 7 exons.

Transcript ENST00000613821 is excluded, because it shares less exons with other transcripts.

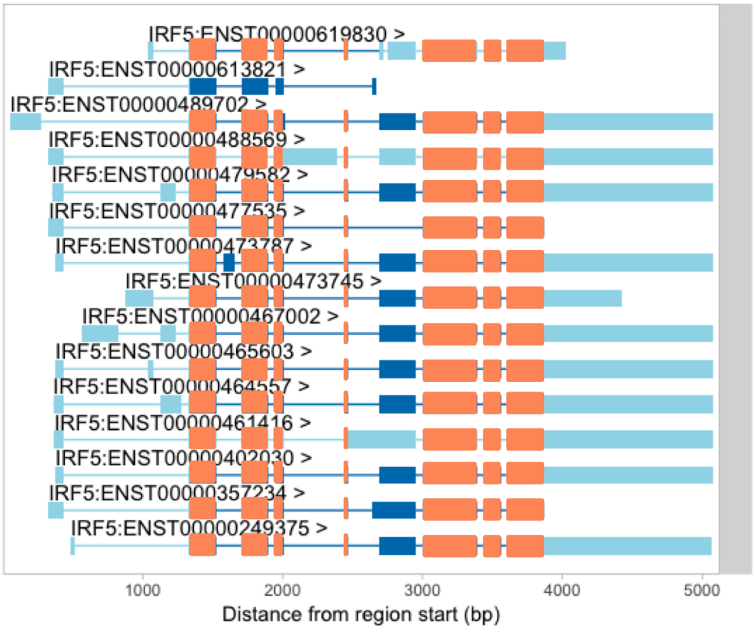

Group 2: All 15 transcripts share 3 exons.

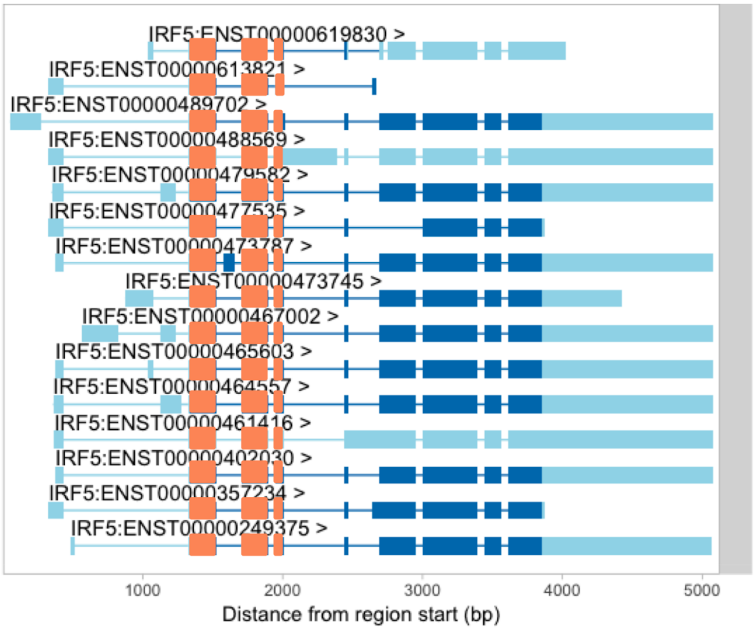

Figure S3 Before we can use txrevise to stratify transcripts into events, we need to identify a subset of transcripts that all share at least one exon. IRF5 has three exons that are shared between all of the transcripts and so we could use those as a scaffold for txrevise to construct independent transcriptional events (group 2). However, some genes do not have any exons that are shared across all transcripts. In that case, it might be preferential to choose the largest subset of transcripts that share the most exons (group 1). Furthermore, even in the case of IRF5, one transcript (ENST00000613821) is much shorter than others and excluding it might lead to better stratification of transcripts into alternative promoter, internal exon and 3' end events (group 1).

A Original promoters of the IRF2 gene

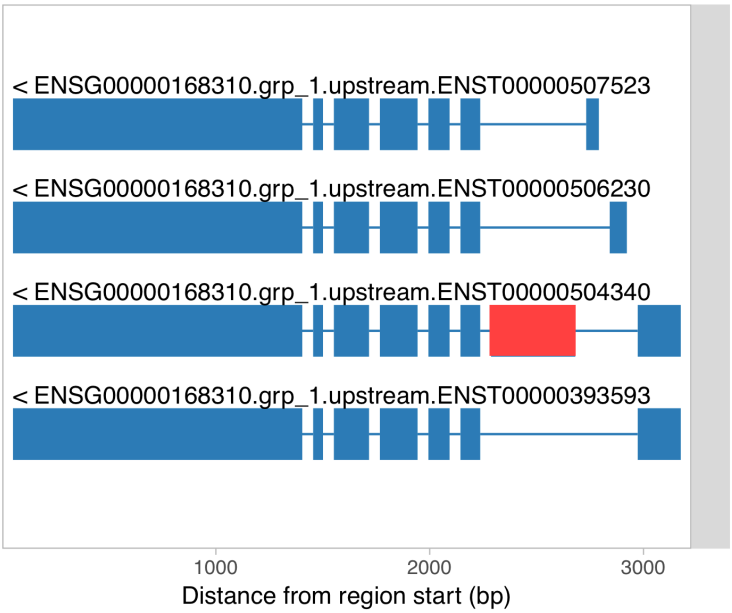

B IRF2 promoters without alternative middle exons

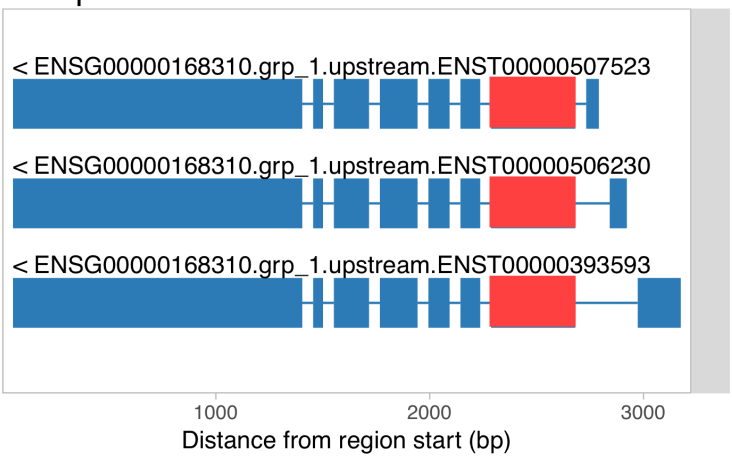

Figure S4 Filling in alternative internal exons for promoter and 3' end events. (**A**) Original transcript start events constructed by txrevise contains an alternative second exon. (**B**) To construct promoter events, the alternative second exon is added into all transcripts and redundant transcripts are removed.

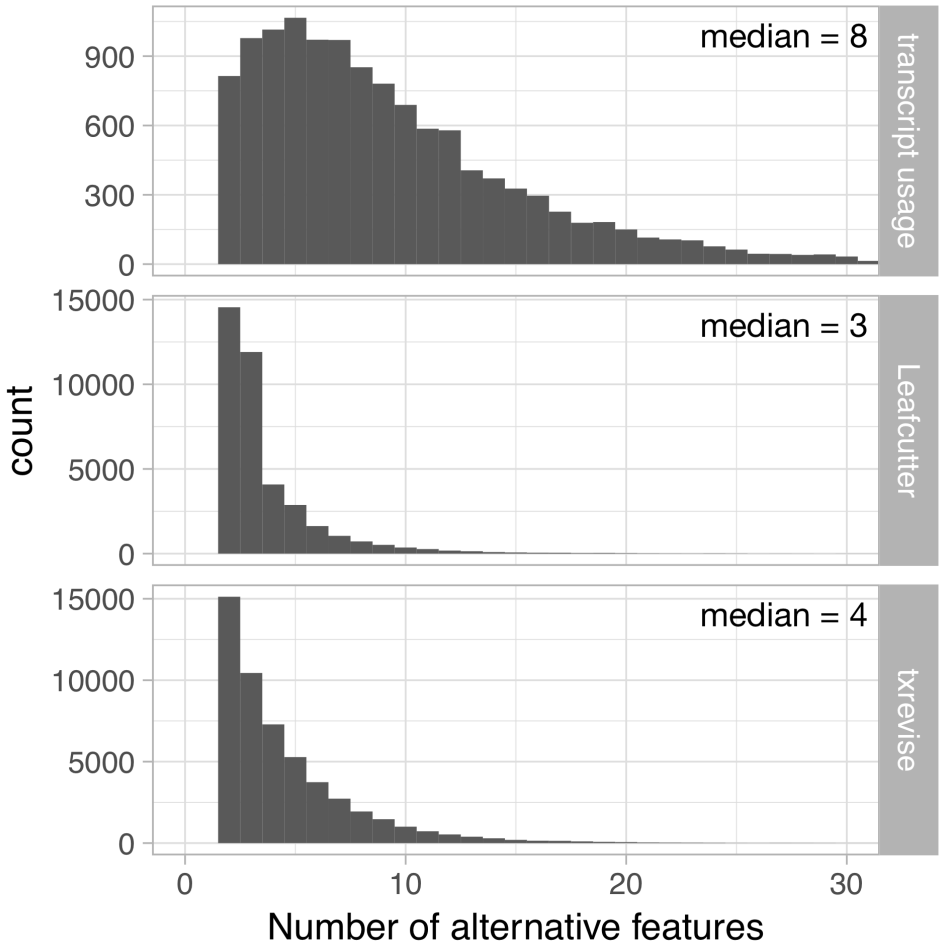

Figure S5 Number of alternative features simultaneously considered by the three transcript-level quantification approaches. For full-length transcript usage, the feature are annotated alternative transcripts. For Leafcutter, the features are alternative intron excision events in a cluster. For txrevise, the features are the alternative transcriptional events within a group (assessed separately for promoters, internal exons or 3' ends). Note that both Leafcutter and txrevise consider multiple groups of events per gene and can thus detect multiple associations per gene.

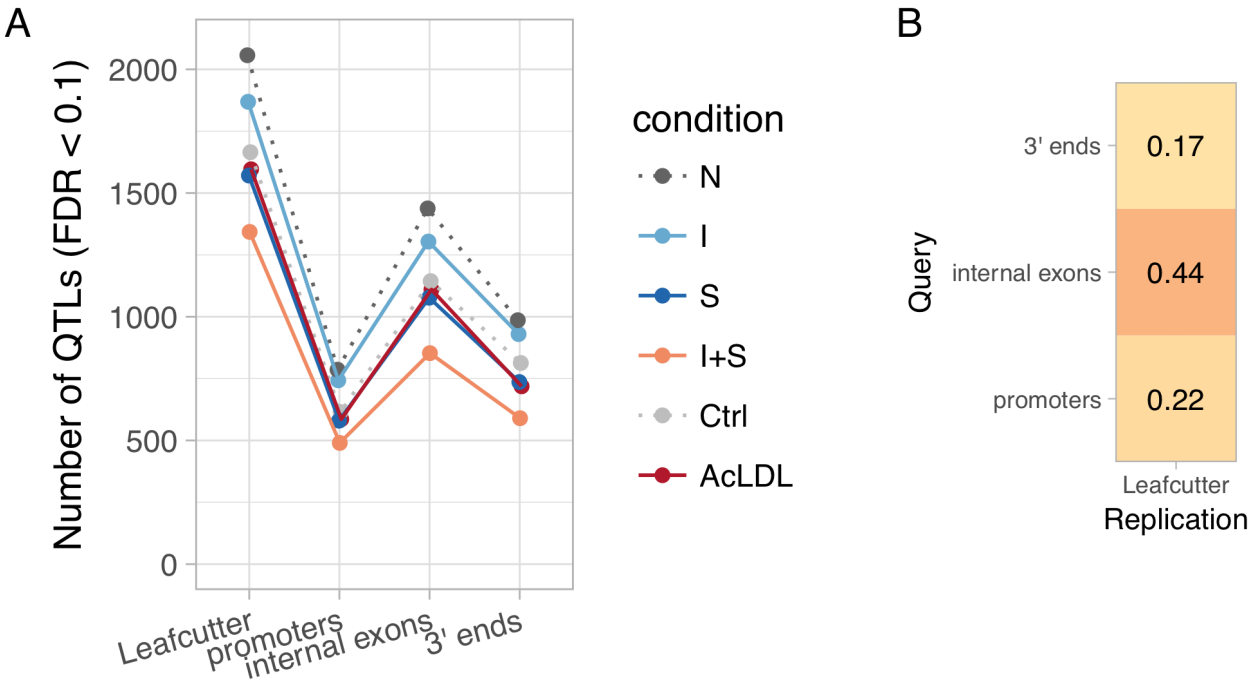

Figure S6 Diversity of transcript usage QTLs. (**A**) Number of detected transcript usage QTLs affecting exon-exon junction usage (Leafcutter) or different parts of the transcript (promoters, internal exons, 3' ends) in each experimental condition. (**B**) Fraction of txrevise promoter, internal exon and 3' end usage QTLs that were replicated by Leafcutter (lead variant within R^2 > 0.8 for the same gene; see Methods).

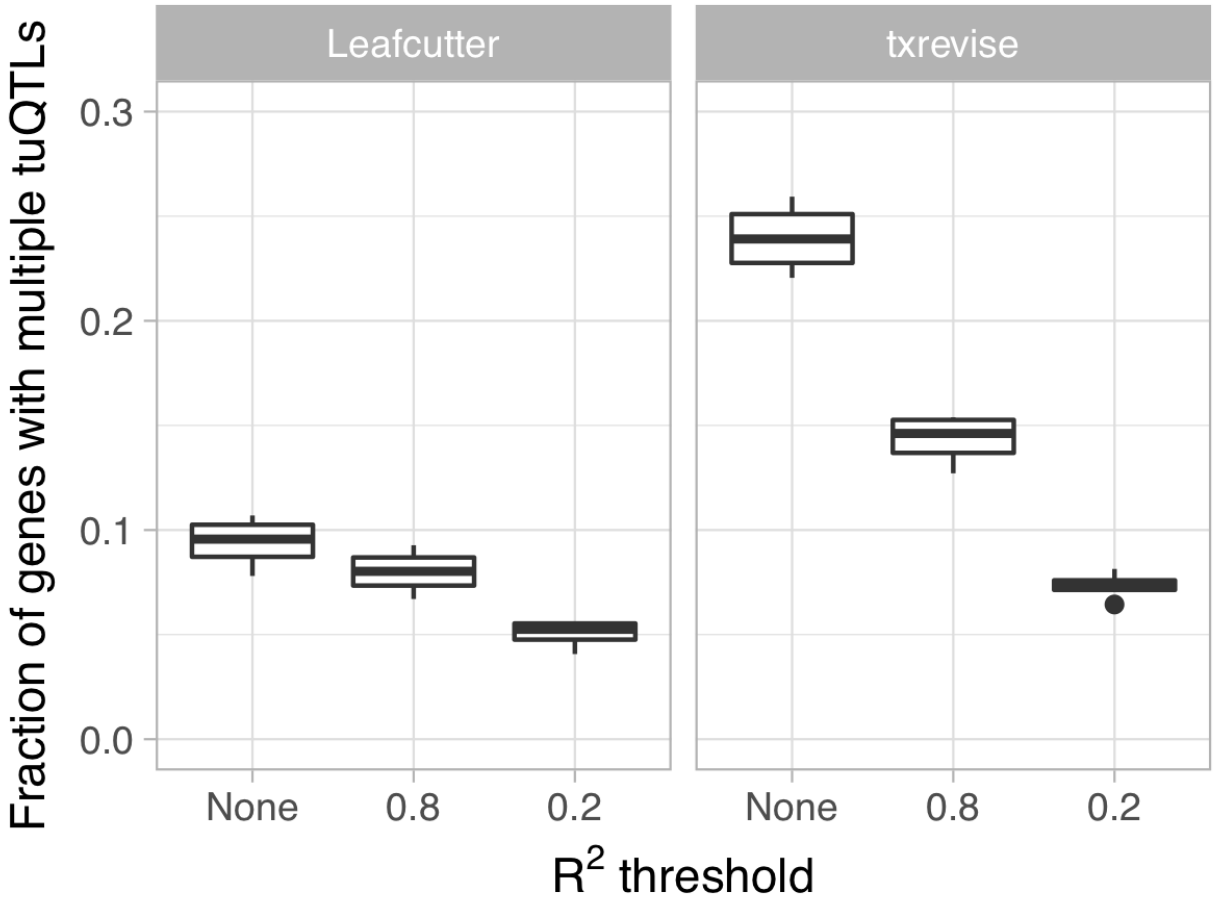

Figure S7 Fraction of genes with multiple independent tuQTLs detected by Leafcutter and txrevise**.** We first identified all tuQTLs for the same gene at the same 10% FDR threshold and then ascertained their independence by thresholding on LD at two levels of stringency ($R^2 < 0.2$ or $R^2 < 0.8$).

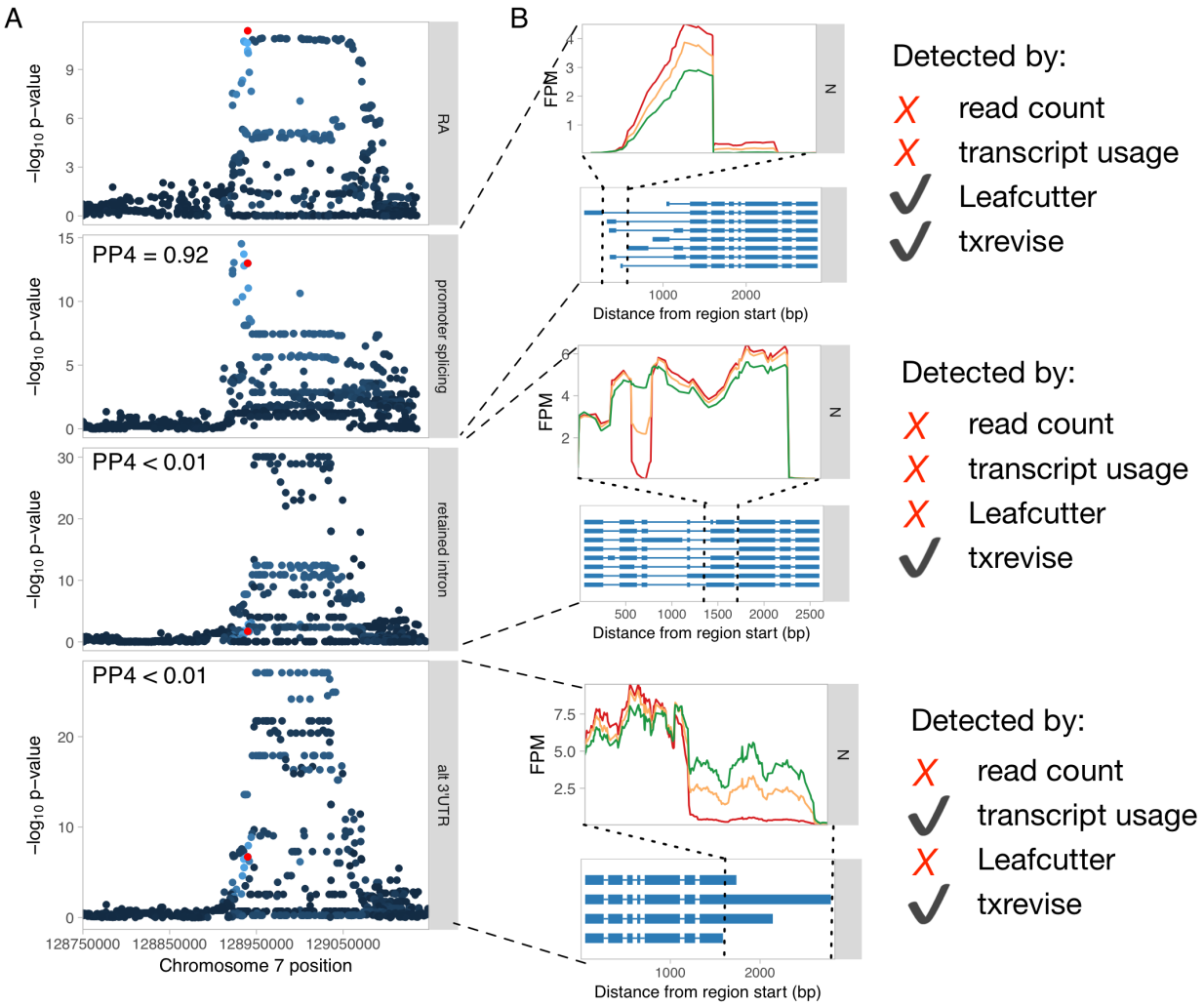

Figure S8 Genetics of transcript usage of IRF5 gene. (**A**) Three independent tuQTLs for IRF5 regulating splicing in the first exon, intron retention in coding exon 5 and 3' UTR length. PP4 represents the posterior probability from coloc [32] that the GWAS and QTL signals share a single causal variant. Only the promoter splicing QTL colocalises with a GWAS hit for rheumatoid arthritis (RA) [30] (PP4 = 0.92). (**D**) RNA-seq read coverage plots of the three tuQTLs stratified by the genotypes of the lead variants. Only txrevise detected all three tuQTLs. Leafcutter only detected the first splicing event, because the other two did not manifest at level of junction reads. Similarly, full-length transcript usage analysis only detected the polyadenylation event, because it had the largest effect size.

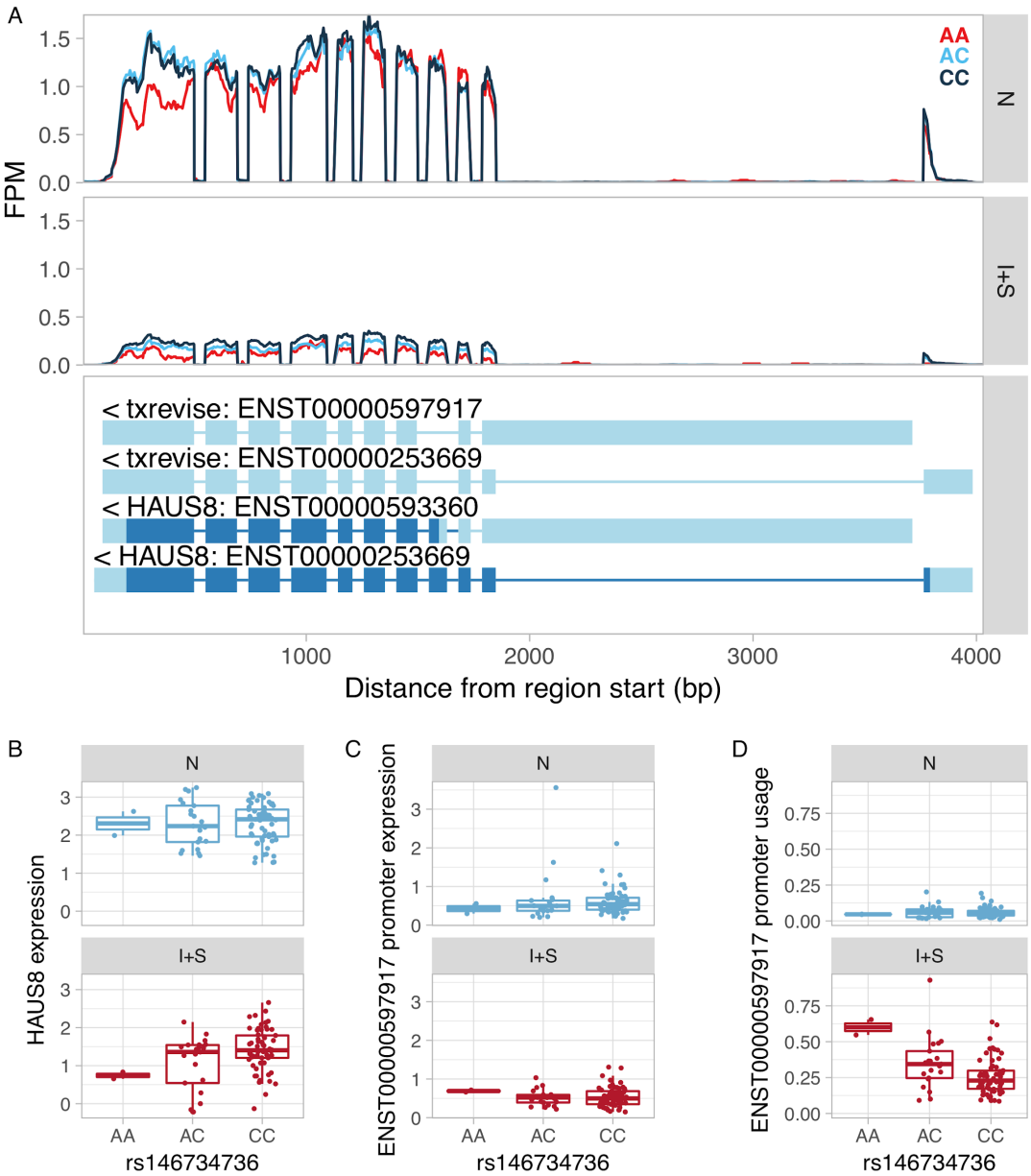

Figure S9: Example of an apparent transcript usage QTL caused by an IFNɣ + *Salmonella* specific eQTL. (**A**) RNA-seq read coverage plot of the HAUS8 gene stratified by the genotype of the lead eQTL variant. FPM, fragments per million. (**B**) The rs146734736 variant is an IFNɣ + Salmonella-specific eQTL for the HAUS8 gene, regulating its total gene expression level. (**C**) The lead eQTL variant is not associated with the absolute expression of the alternative promoter of the gene (ENST00000597917). Furthermore, the average expression of the transcript with the alternative promoter is below 1 TPM, suggesting that it is either not expressed or expressed at very low background expression levels. (**D**) Since the rs146734736 variant is associated with total expression level of the gene, but not with the absolute expression level of the ENST00000597917 transcript, it appears to be associated with the *relative* expression of the ENST00000597917 transcript.

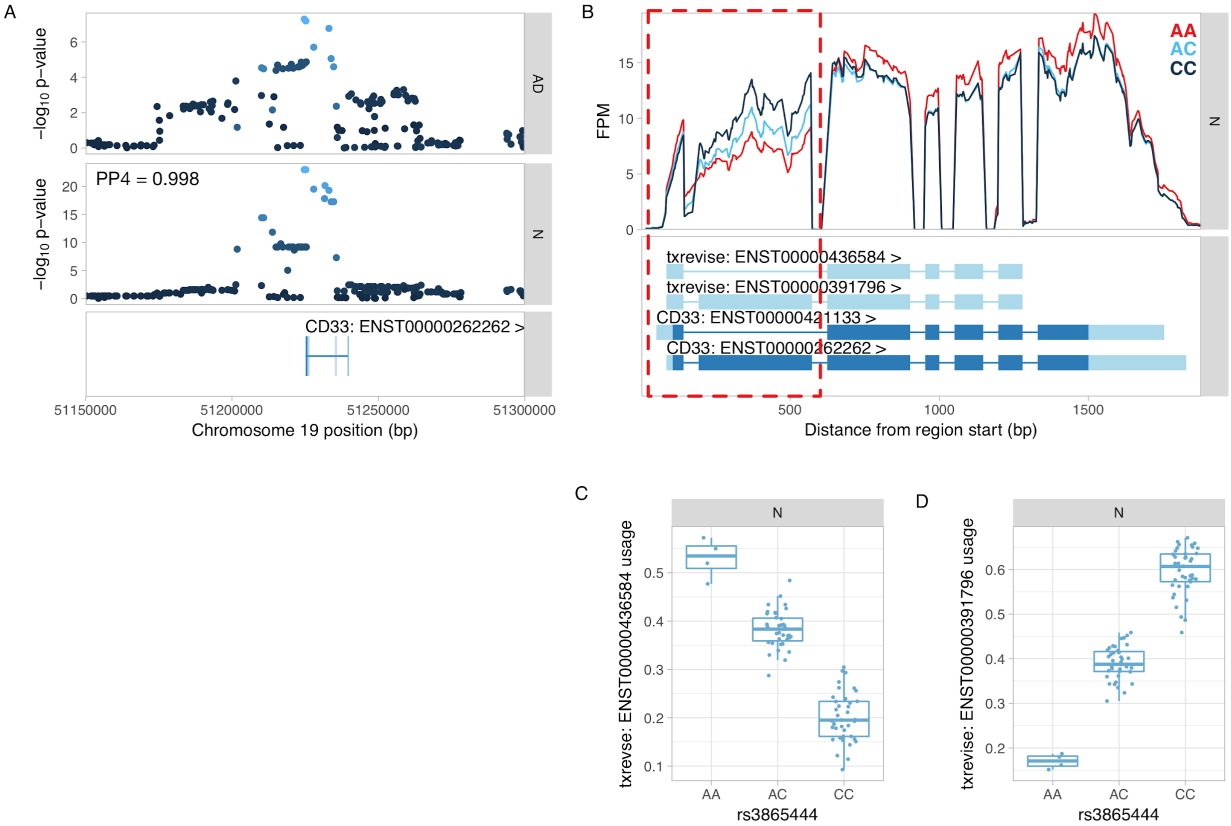

Figure S10 Colocalisation between *CD33* splicing QTL (sQTL) and GWAS hit for Alzheimer's disease (AD). (**A**) Manhattan plots of the Alzheimer's disease GWAS hit [56] and a sQTL for *CD33*. PP4 represents the posterior probability from coloc [32] that the GWAS and sQTL signals share a single causal variant. (**B**) Read coverage plot of the of the CD33 gene stratified by the genotype of the lead sQTL variant (rs3865444). The alternatively spliced exon 2 is highlighted by the red rectangle. Ensembl transcript annotations falsely link skipped exon 2 to alternative 5' and 3' UTRs although these do not appear to be regulated by the sQTL variant. FPM, fragments per million. (**C**) Usage of the *CD33* transcript with skipped exon 2 stratified by the lead sQTL variant. (**D**) Usage of the *CD33* transcript containing exon 2 stratified by the lead sQTL variant.

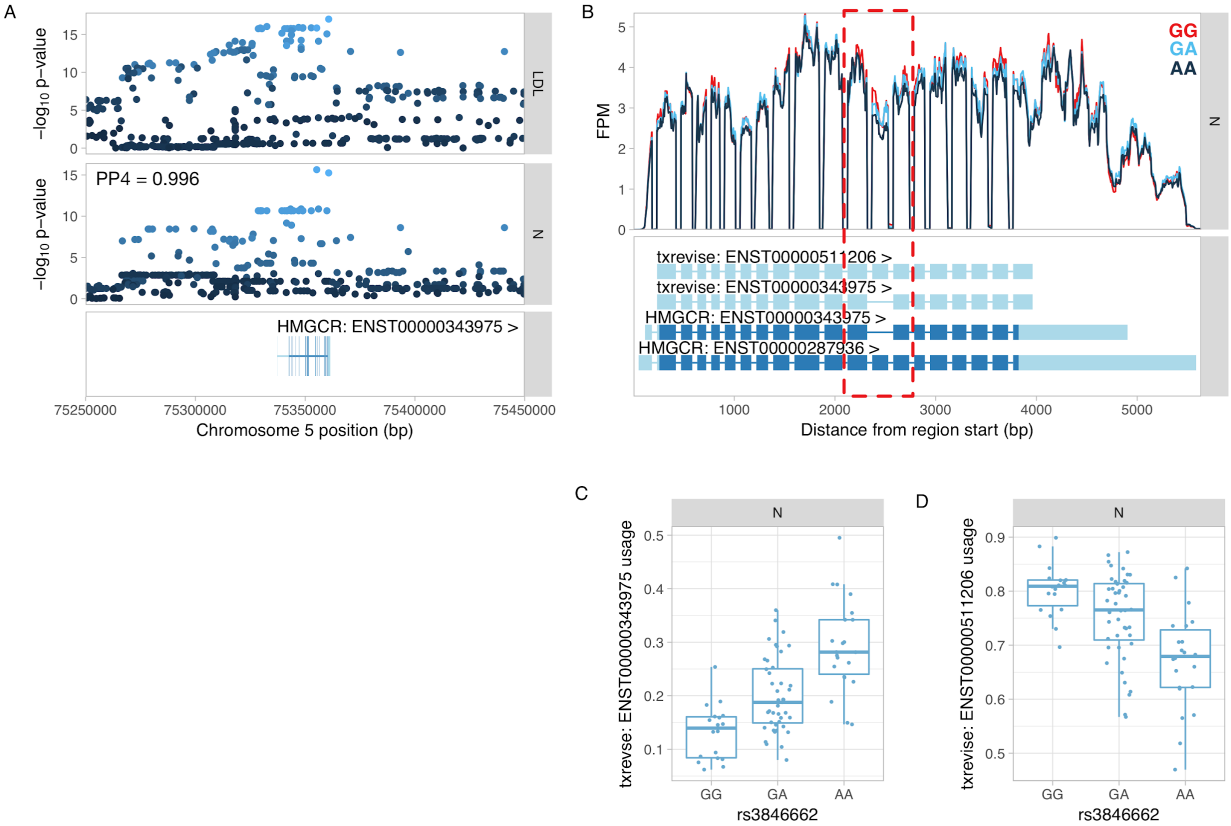

Figure S11 Colocalisation between *HMGCR* splicing QTL (sQTL) and GWAS hit for LDL. (**A**) Manhattan plots of the LDL GWAS hit [66] and an sQTL for *HMGCR*. PP4 represents the posterior probability from coloc [32] that the GWAS and sQTL signals share a single causal variant. (**B**) Read coverage plot of the of the HMGCR gene stratified by the genotype of the lead sQTL variant (rs3846662). The alternatively spliced exon 13 is highlighted by the red rectangle. Ensembl transcript annotations falsely link skipped exon 13 to alternative 5' and 3' UTRs although these do not appear to be differentially regulated by the sQTL variant. FPM, fragments per million. (**C**) Usage of the *HMGCR* transcript with skipped exon 13 stratified by the lead sQTL variant. (**D**) Usage of the *HMGCR* transcript containing exon 13 stratified by the lead sQTL variant.

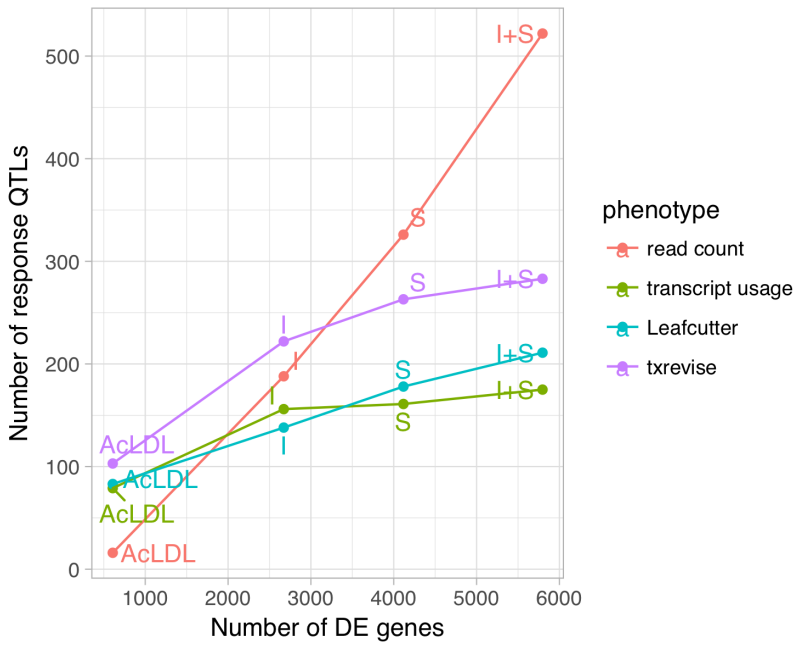

Figure S12 Relationship between the number of differential expressed genes in each condition and number of response QTLs detected in that condition.

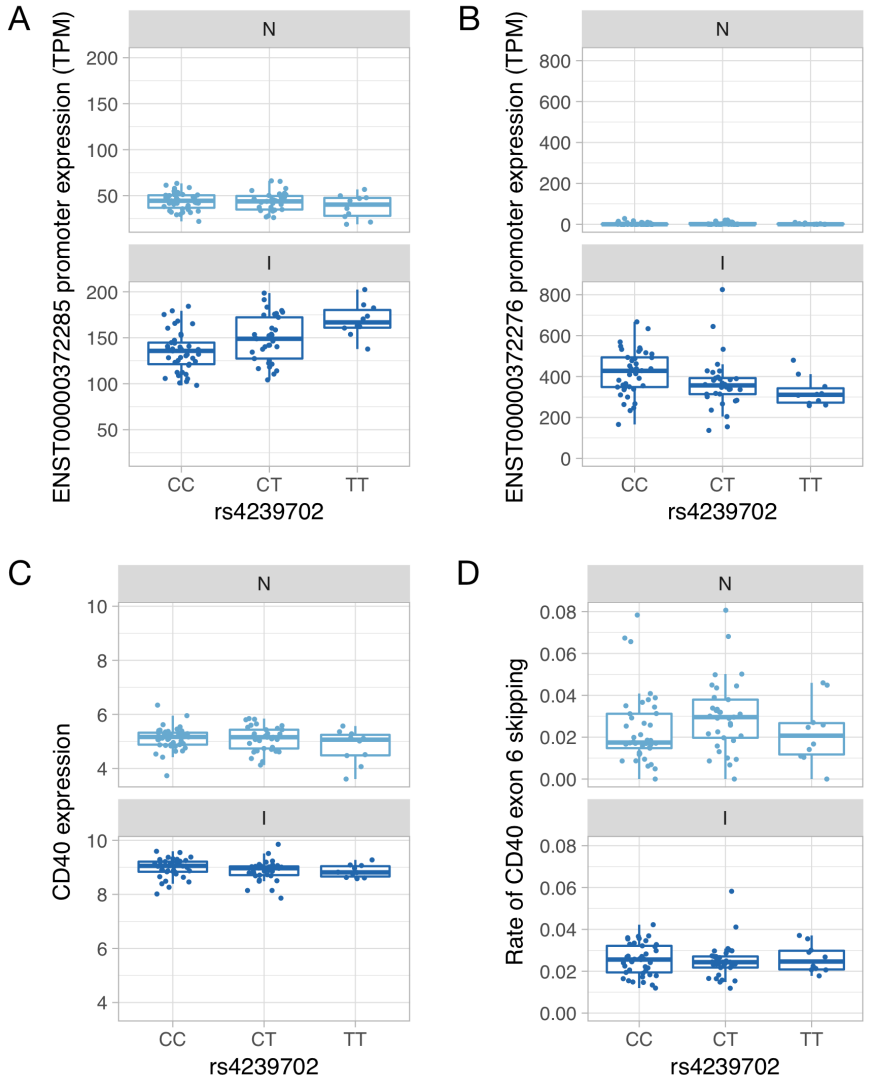

Figure S13 Genetics of *CD40* expression**.** (**A**) Absolute expression of the ENST00000372285 promoter in TPM units stratified by the genotype of the rs4239702 variant. (**B**) Absolute expression of the ENST00000372276 promoter in TPM units stratified by the genotype of the rs4239702 variant. (**C**) Normalized CD40 read count stratified by the genotype of the rs4239702 variant. (**D**) Rate of CD40 exon 6 skipping stratified by the genotype of the rs4239702 variant.

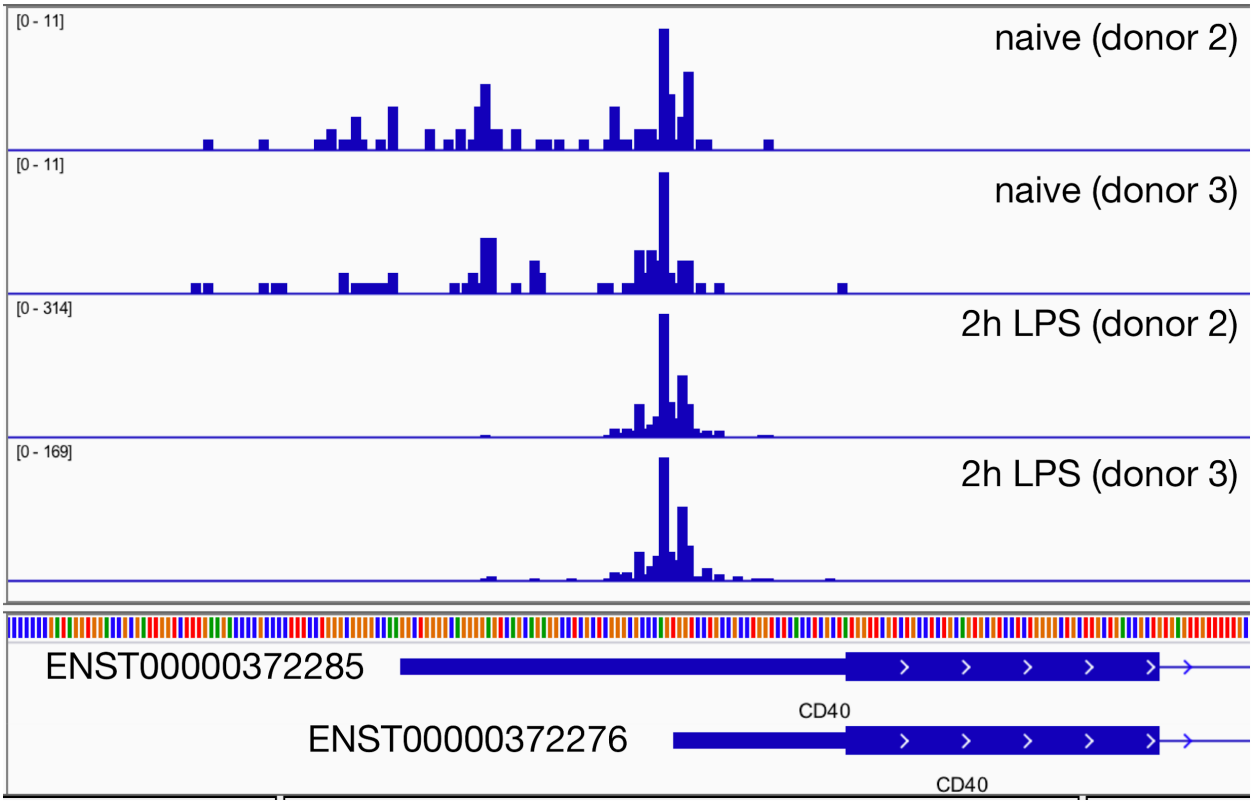

Figure S14 Read coverage of the Cap Analysis of Gene Expression (CAGE) data from two replicates of monocyte-derived macrophages before and after 2h stimulation with lipopolysaccharide (LPS). The data was generated by the FANTOM5 consortium [31]. The promoter containing the short 5' UTR is strongly upregulated after 2h LPS stimulation.

References

1. Kim-Hellmuth S, Bechheim M, Pütz B, Mohammadi P, Nédélec Y, Giangreco N, et al. Genetic regulatory effects modified by immune activation contribute to autoimmune disease associations. Nat Commun. 2017;8:266.

2. Fairfax BP, Humburg P, Makino S, Naranbhai V, Wong D, Lau E, et al. Innate immune activity conditions the effect of regulatory variants upon monocyte gene expression. Science. 2014;343:1246949.

3. Alasoo K, Rodrigues J, Mukhopadhyay S, Knights AJ, Mann AL, Kundu K, et al. Shared genetic effects on chromatin and gene expression indicate a role for enhancer priming in immune response. Nat Genet [Internet]. 2018; Available from: https://doi.org/10.1038/s41588-018-0046-7

4. Li YI, van de Geijn B, Raj A, Knowles DA, Petti AA, Golan D, et al. RNA splicing is a primary link between genetic variation and disease. Science. 2016;352:600–4.

5. Li YI, Knowles DA, Humphrey J, Barbeira AN, Dickinson SP, Im HK, et al. Annotation-free quantification of RNA splicing using LeafCutter. Nat Genet. 2018;50:151–8.

6. Pal S, Gupta R, Kim H, Wickramasinghe P, Baubet V, Showe LC, et al. Alternative transcription exceeds alternative splicing in generating the transcriptome diversity of cerebellar development. Genome Res. 2011;21:1260–72.

7. Reyes A, Huber W. Alternative start and termination sites of transcription drive most transcript isoform differences across human tissues. Nucleic Acids Res. 2018;46:582–92.

8. Demircioğlu D, Kindermans M, Nandi T, Cukuroglu E, Calabrese C, Fonseca NA, et al. A pan cancer analysis of promoter activity highlights the regulatory role of alternative transcription start sites and their association with noncoding mutations. bioRxiv. Cold Spring Harbor Labs Journals; 2017;176487.

9. Garieri M, Delaneau O, Santoni F, Fish RJ, Mull D, Carninci P, et al. The effect of genetic variation on promoter usage and enhancer activity. Nat Commun. Nature Publishing Group; 2017;8:1358.

10. Zhernakova DV, de Klerk E, Westra H-J, Mastrokolias A, Amini S, Ariyurek Y, et al. DeepSAGE reveals genetic variants associated with alternative polyadenylation and expression of coding and non-coding transcripts. PLoS Genet. 2013;9:e1003594.

11. Nédélec Y, Sanz J, Baharian G, Szpiech ZA, Pacis A, Dumaine A, et al. Genetic Ancestry and Natural Selection Drive Population Differences in Immune Responses to Pathogens. Cell. 2016;167:657–69.e21.

12. Chen L, Ge B, Casale FP, Vasquez L, Kwan T, Garrido-Martín D, et al. Genetic Drivers of Epigenetic and Transcriptional Variation in Human Immune Cells. Cell. Elsevier; 2016;167:1398–414.e24.

13. Chun YJ, Chen J, Villani A-C, Subramaniam M, Gate RE, Bhangale T, et al. Genetic analysis of isoform usage in the human anti-viral response reveals influenza-specific regulation

of ERAP2 transcripts under balancing selection. bioRxiv. Cold Spring Harbor Laboratory; 2017;188961.

14. Alamancos GP, Pagès A, Trincado JL, Bellora N, Eyras E. Leveraging transcript quantification for fast computation of alternative splicing profiles. RNA. 2015;21:1521–31.

15. Teng M, Love MI, Davis CA, Djebali S, Dobin A, Graveley BR, et al. A benchmark for RNA-seq quantification pipelines. Genome Biol. 2016;17:74.

16. Kanitz A, Gypas F, Gruber AJ, Gruber AR, Martin G, Zavolan M. Comparative assessment of methods for the computational inference of transcript isoform abundance from RNA-seq data. Genome Biol. 2015;16:150.

17. Ongen H, Dermitzakis ET. Alternative Splicing QTLs in European and African Populations. Am J Hum Genet. 2015;97:567–75.

18. Lappalainen T, Sammeth M, Friedländer MR, ’t Hoen PAC, Monlong J, Rivas MA, et al. Transcriptome and genome sequencing uncovers functional variation in humans. Nature. 2013;501:506–11.

19. Fadista J, Vikman P, Laakso EO, Mollet IG, Esguerra JL, Taneera J, et al. Global genomic and transcriptomic analysis of human pancreatic islets reveals novel genes influencing glucose metabolism. Proc Natl Acad Sci U S A. 2014;111:13924–9.

20. Vaquero-Garcia J, Barrera A, Gazzara MR, González-Vallinas J, Lahens NF, Hogenesch JB, et al. A new view of transcriptome complexity and regulation through the lens of local splicing variations. Elife. 2016;5:e11752.

21. Patro R, Duggal G, Love MI, Irizarry RA, Kingsford C. Salmon provides fast and bias-aware quantification of transcript expression. Nat Methods. 2017;14:417–9.

22. Liao Y, Smyth GK, Shi W. featureCounts: an efficient general purpose program for assigning sequence reads to genomic features. Bioinformatics. Oxford Univ Press; 2014;30:923–30.

23. Bentley DL. Coupling mRNA processing with transcription in time and space. Nat Rev Genet. 2014;15:163–75.

24. Anvar SY, Allard G, Tseng E, Sheynkman GM, de Klerk E, Vermaat M, et al. Full-length mRNA sequencing uncovers a widespread coupling between transcription initiation and mRNA processing. Genome Biol. 2018;19:46.

25. Gruber AJ, Schmidt R, Gruber AR, Martin G, Ghosh S, Belmadani M, et al. A comprehensive analysis of 3′ end sequencing data sets reveals novel polyadenylation signals and the repressive role of heterogeneous ribonucleoprotein C on cleavage and polyadenylation. Genome Res. 2016;26:1145–59.

26. Van Nostrand EL, Freese P, Pratt GA, Wang X, Wei X, Blue SM, et al. A Large-Scale Binding and Functional Map of Human RNA Binding Proteins. bioRxiv. Cold Spring Harbor Labs Journals; 2017;179648.

27. Pickrell JK. Joint analysis of functional genomic data and genome-wide association studies of 18 human traits. Am J Hum Genet. 2014;94:559–73.

28. Malik M, Simpson JF, Parikh I, Wilfred BR, Fardo DW, Nelson PT, et al. CD33 Alzheimer's risk-altering polymorphism, CD33 expression, and exon 2 splicing. J Neurosci. 2013;33:13320–5.

29. Burkhardt R, Kenny EE, Lowe JK, Birkeland A, Josowitz R, Noel M, et al. Common SNPs in HMGCR in micronesians and whites associated with LDL-cholesterol levels affect alternative splicing of exon13. Arterioscler Thromb Vasc Biol. 2008;28:2078–84.

30. Okada Y, Wu D, Trynka G, Raj T, Terao C, Ikari K, et al. Genetics of rheumatoid arthritis contributes to biology and drug discovery. Nature. 2014;506:376–81.

31. Baillie JK, Arner E, Daub C, De Hoon M, Itoh M, Kawaji H, et al. Analysis of the human monocyte-derived macrophage transcriptome and response to lipopolysaccharide provides new insights into genetic aetiology of inflammatory bowel disease. PLoS Genet. 2017;13:e1006641.

32. Giambartolomei C, Vukcevic D, Schadt EE, Franke L, Hingorani AD, Wallace C, et al. Bayesian Test for Colocalisation between Pairs of Genetic Association Studies Using Summary Statistics. PLoS Genet. 2014;10:e1004383.

33. Katz Y, Wang ET, Airoldi EM, Burge CB. Analysis and design of RNA sequencing experiments for identifying isoform regulation. Nat Methods. 2010;7:1009–15.

34. Sterne-Weiler T, Weatheritt RJ, Best A, Ha KCH, Blencowe BJ. Whippet: an efficient method for the detection and quantification of alternative splicing reveals extensive transcriptomic complexity. bioRxiv. Cold Spring Harbor Labs Journals; 2017;158519.

35. FANTOM Consortium and the RIKEN PMI and CLST (DGT), Forrest ARR, Kawaji H, Rehli M, Baillie JK, de Hoon MJL, et al. A promoter-level mammalian expression atlas. Nature. 2014;507:462–70.

36. Pertea M, Pertea GM, Antonescu CM, Chang T-C, Mendell JT, Salzberg SL. StringTie enables improved reconstruction of a transcriptome from RNA-seq reads. Nat Biotechnol. Nature Publishing Group; 2015;33:290–5.

37. Alasoo K. wiggleplotr: Make read coverage plots from BigWig files [Internet]. Bioconductor; 2017 [cited 2017 Dec 13]. Available from: http://bioconductor.org/packages/release/bioc/html/wiggleplotr.html

38. Odhams CA, Cunninghame Graham DS, Vyse TJ. Profiling RNA-Seq at multiple resolutions markedly increases the number of causal eQTLs in autoimmune disease. PLoS Genet. 2017;13:e1007071.

39. GTEx Consortium, Laboratory, Data Analysis &Coordinating Center (LDACC)—Analysis Working Group, Statistical Methods groups—Analysis Working Group, Enhancing GTEx (eGTEx) groups, NIH Common Fund, NIH/NCI, et al. Genetic effects on gene expression across human tissues. Nature. Nature Publishing Group; 2017;550:204–13.

40. Kilpinen H, Goncalves A, Leha A, Afzal V, Alasoo K, Ashford S, et al. Common genetic variation drives molecular heterogeneity in human iPSCs. Nature. 2017;546:370–5.

41. Dobin A, Davis CA, Schlesinger F, Drenkow J, Zaleski C, Jha S, et al. STAR: ultrafast universal RNA-seq aligner. Bioinformatics. 2013;29:15–21.

42. Jun G, Flickinger M, Hetrick KN, Romm JM, Doheny KF, Abecasis GR, et al. Detecting and estimating contamination of human DNA samples in sequencing and array-based genotype data. Am J Hum Genet. 2012;91:839–48.

43. Wagner GP, Kin K, Lynch VJ. Measurement of mRNA abundance using RNA-seq data: RPKM measure is inconsistent among samples. Theory Biosci. 2012;131:281–5.

44. Hansen KD, Irizarry RA, Wu Z. Removing technical variability in RNA-seq data using conditional quantile normalization. Biostatistics. 2012;13:204–16.

45. Ellis SE, Gupta S, Ashar FN, Bader JS, West AB, Arking DE. RNA-Seq optimization with eQTL gold standards. BMC Genomics. 2013;14:892.

46. Soneson C, Love MI, Robinson MD. Differential analyses for RNA-seq: transcript-level estimates improve gene-level inferences. F1000Res [Internet]. 2015 [cited 2015 Dec 30];4. Available from: http://f1000research.com/articles/4-1521/v1/pdf

47. Lawrence M, Huber W, Pagès H, Aboyoun P, Carlson M, Gentleman R, et al. Software for computing and annotating genomic ranges. PLoS Comput Biol. 2013;9:e1003118.

48. Durinck S, Moreau Y, Kasprzyk A, Davis S, De Moor B, Brazma A, et al. BioMart and Bioconductor: a powerful link between biological databases and microarray data analysis. Bioinformatics. 2005;21:3439–40.

49. Zhao H, Sun Z, Wang J, Huang H, Kocher J-P, Wang L. CrossMap: a versatile tool for coordinate conversion between genome assemblies. Bioinformatics. 2014;30:1006–7.

50. Zheng X, Levine D, Shen J, Gogarten SM, Laurie C, Weir BS. A high-performance computing toolset for relatedness and principal component analysis of SNP data. Bioinformatics. 2012;28:3326–8.

51. Delaneau O, Ongen H, Brown AA, Fort A, Panousis NI, Dermitzakis ET. A complete tool set for molecular QTL discovery and analysis. Nat Commun. Nature Publishing Group; 2017;8:15452.

52. Zerbino DR, Achuthan P, Akanni W, Amode MR, Barrell D, Bhai J, et al. Ensembl 2018. Nucleic Acids Res. 2018;46:D754–61.

53. Van Nostrand EL, Pratt GA, Shishkin AA, Gelboin-Burkhart C, Fang MY, Sundararaman B, et al. Robust transcriptome-wide discovery of RNA-binding protein binding sites with enhanced CLIP (eCLIP). Nat Methods. 2016;13:508–14.

54. Jones E, Oliphant T, Peterson P. {SciPy}: Open source scientific tools for {Python} [Internet]. citeulike.org; 2001--. Available from: http://www.scipy.org

55. Liu JZ, van Sommeren S, Huang H, Ng SC, Alberts R, Takahashi A, et al. Association analyses identify 38 susceptibility loci for inflammatory bowel disease and highlight shared genetic risk across populations. Nat Genet. 2015;47:979–86.

56. Lambert JC, Ibrahim-Verbaas CA, Harold D, Naj AC, Sims R, Bellenguez C, et al. Meta-analysis of 74,046 individuals identifies 11 new susceptibility loci for Alzheimer's disease. Nat Genet. 2013;45:1452–8.

57. Bentham J, Morris DL, Cunninghame Graham DS, Pinder CL, Tombleson P, Behrens TW, et al. Genetic association analyses implicate aberrant regulation of innate and adaptive immunity genes in the pathogenesis of systemic lupus erythematosus. Nat Genet. 2015;47:1457–64.

58. Onengut-Gumuscu S, Chen W-M, Burren O, Cooper NJ, Quinlan AR, Mychaleckyj JC, et al. Fine mapping of type 1 diabetes susceptibility loci and evidence for colocalization of causal variants with lymphoid gene enhancers. Nat Genet. 2015;47:381–6.

59. Schizophrenia Working Group of the Psychiatric Genomics Consortium. Biological insights from 108 schizophrenia-associated genetic loci. Nature. 2014;511:421–7.

60. International Multiple Sclerosis Genetics Consortium (IMSGC), Beecham AH, Patsopoulos NA, Xifara DK, Davis MF, Kemppinen A, et al. Analysis of immune-related loci identifies 48 new susceptibility variants for multiple sclerosis. Nat Genet. 2013;45:1353–60.

61. Trynka G, Hunt KA, Bockett NA, Romanos J, Mistry V, Szperl A, et al. Dense genotyping identifies and localizes multiple common and rare variant association signals in celiac disease. Nat Genet. 2011;43:1193–201.

62. Faraco J, Lin L, Kornum BR, Kenny EE, Trynka G, Einen M, et al. ImmunoChip study implicates antigen presentation to T cells in narcolepsy. PLoS Genet. 2013;9:e1003270.

63. Morris AP, Voight BF, Teslovich TM, Ferreira T, Segrè AV, Steinthorsdottir V, et al. Large-scale association analysis provides insights into the genetic architecture and pathophysiology of type 2 diabetes. Nat Genet. 2012;44:981–90.

64. Nikpay M, Goel A, Won H-H, Hall LM, Willenborg C, Kanoni S, et al. A comprehensive 1,000 Genomes-based genome-wide association meta-analysis of coronary artery disease. Nat Genet. 2015;47:1121–30.

65. Nelson CP, Goel A, Butterworth AS, Kanoni S, Webb TR, Marouli E, et al. Association analyses based on false discovery rate implicate new loci for coronary artery disease. Nat Genet. 2017;49:1385–91.

66. Iotchkova V, Huang J, Morris JA, Jain D, Barbieri C, Walter K, et al. Discovery and refinement of genetic loci associated with cardiometabolic risk using dense imputation maps. Nat Genet. Nature Research; 2016;48:1303–12.

67. Guo H, Fortune MD, Burren OS, Schofield E, Todd JA, Wallace C. Integration of disease association and eQTL data using a Bayesian colocalisation approach highlights six candidate causal genes in immune-mediated diseases. Hum Mol Genet. 2015;24:3305–13.

68. Conway JR, Lex A, Gehlenborg N. UpSetR: an R package for the visualization of intersecting sets and their properties. Bioinformatics. 2017;33:2938–40.

69. Köster J, Rahmann S. Snakemake--a scalable bioinformatics workflow engine. Bioinformatics. 2012;28:2520–2.